

**AN INVESTIGATION INTO THE LIMITATIONS OF THE
HARMONIC APPROXIMATION IN THE CALCULATION
OF VIBRATIONAL ISOTOPIC SHIFTS**

by

Guillermo García

Bachelor of Science, 2000
Universidad Autónoma de Zacatecas
Zacatecas, Mexico

Submitted to the Graduate Faculty of the
College of Science and Engineering
Texas Christian University
in partial fulfillment of the requirements
for the degree of

Doctor of Philosophy

August 2008

Acknowledgements

I had the fortune to have as an adviser a wise physicist who is also an admirable person, Dr. C. M. L. Rittby. Working with Dr. W. R. M. Graham was simply a pleasure too. I want to express all of my gratitude, respect, and admiration to both of them.

I also want to thank to Cassidy Smith and Stephen Nauyoks for helping me to revise this work with respect to my English grammar and syntax.

In Spanish (to my parents):

Mi trabajo se lo dedico a Martha y Guillermo, mis padres, porque yo les debo todo. Gracias por su apoyo. Tambien gracias a Alejandro...por ser la pura sabrosura.

TABLE OF CONTENTS:

ACKNOWLEDGEMENTS	ii
LIST OF TABLES.....	iv
LIST OF FIGURES.....	v
CHAPTER I. INTRODUCTION	1
CHAPTER II. THEORETICAL FRAMEWORK	10
2.1. THE HARMONIC APPROXIMATION	10
2.1.1. <i>Vibrational Frequencies and the “Exact” Calculation of Isotopic Shifts</i>	12
2.2. RAYLEIGH-SCHRÖDINGER PERTURBATION THEORY	13
2.3. OCCUPATION NUMBER REPRESENTATION	16
2.4. ISOTOPIC SUBSTITUTION AS A MASS PERTURBATION	19
2.4.1. <i>First Order Treatment</i>	21
2.4.2. <i>Second Order Treatment</i>	22
2.4.3. <i>Self-Shift to Infinite Order</i>	24
CHAPTER III. MODE INTERACTION	26
3.1. INTRODUCTION	26
3.2. METHOD	27
3.2.1. <i>Application of the Mirror Transformation to Experimental Isotopic Shifts</i>	31
3.2.2. <i>Isotopic Deperturbation Method</i>	32
3.3. APPLICATION OF ISOTOPIC DEPERTURBATION METHOD TO LINEAR CARBON CHAINS	33
3.3.1. <i>Linear C_n (n = 3 – 6)</i>	34
3.3.2. <i>Linear C_n (n = 7 – 12)</i>	41
3.3.3. <i>Linear C_n (n = 15, 18)</i>	49
3.4. CONCLUSIONS.....	51
CHAPTER IV. ANHARMONICITY	53
4.1. INTRODUCTION	53
4.2. THEORY	54
4.2.1. <i>Derivation of Mass-Reduced Perturbation Expressions</i>	54
4.2.2. <i>Mass Scaling of RSPT for Harmonic Oscillators</i>	56
4.2.3. <i>Derivation of Anharmonic Isotopic Shift Expressions</i>	59
4.3. APPLICATION AND DISCUSSION	60
4.4. CONCLUSIONS.....	69
CHAPTER V. CONCLUSIONS AND FUTURE WORK.....	70
5.1. CONCLUSIONS.....	70
5.2. FUTURE WORK	71
APPENDICES	72
A. THE CANONICAL TRANSFORMATION OF THE VIBRATIONAL HAMILTONIAN	72
B. PERTURBATION IN THE NUMBER REPRESENTATION AND NORMAL ORDERED OPERATORS	75
C. DERIVATION OF THE FIRST ORDER CORRECTION TO AN ISOTOPIC SHIFT	80
D. DERIVATION OF THE SECOND ORDER CORRECTION TO AN ISOTOPIC SHIFT	82
E. BRACKETING THEOREM	89
REFERENCES	91
ABSTRACT	
VITA	

LIST OF TABLES

Table 1. Normal mode displacements and harmonic frequencies of the stretching modes of linear C ₃ , calculated at the DFT/B3LYP level with the cc-pVDZ basis set.	37
Table 2. Comparison of values of the anharmonicity from calculation and experiment. All values are in cm ⁻¹	65

LIST OF FIGURES

Figure 1. Application of the isotopic deperturbation method to the isotopic spectra of the $\nu_3(\sigma_u)$ mode of linear C_3	36
Figure 2. Application of the isotopic deperturbation method to the isotopic spectra of the $\nu_7(\sigma_u)$ mode of linear C_{12} : Isotopic shifts due to substitutions on the first (c1) and second (c2) molecular sites.....	42
Figure 3. Application of the isotopic deperturbation method to the isotopic spectra of the $\nu_7(\sigma_u)$ mode of linear C_{12} : Isotopic shifts due to substitution on the third (c3) molecular site.....	44
Figure 4. Application of the isotopic deperturbation method to the isotopic spectra of the $\nu_7(\sigma_u)$ mode of linear C_{12} : Isotopic shifts due to substitution on the fourth (c4) molecular site.....	46
Figure 5. Application of the isotopic deperturbation method to the isotopic spectra of the $\nu_7(\sigma_u)$ mode of linear C_{12} : Isotopic shifts due to substitution on the fifth (c5) molecular site.....	47
Figure 6. Application of the isotopic deperturbation method to the isotopic spectra of the $\nu_7(\sigma_u)$ mode of linear C_{12} : Isotopic shifts due to substitution on the sixth (c6) molecular site.....	48
Figure 7. Comparison between the experimental and simulated isotopic spectra of the $\nu_{10}(\sigma_u)$ mode of linear C_{15} and the $\nu_{12}(\sigma_u)$ mode of linear C_{18} . Carbon ratio: 10% ^{12}C / 90% ^{13}C	49
Figure 8. Comparison between the experimental and simulated isotopic spectra of the $\nu_{12}(\sigma_u)$ mode of linear C_{18} . Carbon ratio: 90% ^{12}C / 10% ^{13}C	50

Figure 9. Experimental (top) and DFT simulated (bottom) isotopic spectra for linear C₃.
The isotopic identification for each absorption is given in parenthesis next to the
experimental frequency..... 61

Figure 10. Experimentally derived (open circles) estimates of the anharmonicity for the
most intense fundamentals of linear carbon chains C_{2n+1}. Filled circles correspond to the
B3LYP/cc-pVDZ results in this work. Triangles refer to existing theoretical predictions in
the literature (see Table 2 for details). 67

Figure 11. Experimentally observed stretching fundamental frequencies for linear carbon
chains C_{2n+1} (n=1-4) vs. the calculated anharmonic B3LYP/cc-pVDZ frequency using the
data in Table 2 (filled circles). The open circles represent the same data for the observed
fundamentals of linear C₁₁ and C₁₃ (see text for discussion). 68

CHAPTER I. INTRODUCTION

Quantum chemistry is a field where quantum theory is applied to the interactions of electrons and nuclei in order to understand the formation and behavior of molecular systems.^{1,2} In particular, quantum chemical models have been developed in order to solve the electronic many-body problem, which is central for a basic understanding of the formation of molecular bonds and chemistry. Of particular interest for the field of molecular spectroscopy is the ability of quantum chemical models to produce accurate electronic, vibrational, and rotational transition frequencies to be compared with experimental results.³ The gradual evolution in the accuracy of the theoretical methods along with the rapid decrease in cost of large computer calculations/simulations have led to an increasingly synergistic approach in the study of molecular structure.

Of particular interest to the TCU Molecular Physics Laboratory is the ability to accurately predict equilibrium structures and vibrational spectra. To achieve this in a computationally feasible way one commonly invokes the Born-Oppenheimer approximation,^{4,5} which consists of the approximate separation of the electronic and nuclear motions in a molecular system. The total Hamiltonian for the electronic and nuclear motion in the space fixed frame can be written

$$H^{eN}(\mathbf{r}, \mathbf{R}) = -\sum_{\alpha=1}^N \frac{1}{2m_{\alpha}} \nabla_{\alpha}^2 + H^e(\mathbf{r}; \mathbf{R}) \equiv T^{nuc} + H^e(\mathbf{r}; \mathbf{R}) \quad (1.1)$$

where \mathbf{R} denotes all of the nuclear coordinates and \mathbf{r} all of the electronic coordinates.

$H^e(\mathbf{r}; \mathbf{R})$ is the total electronic Hamiltonian

$$H^e(\mathbf{r}; \mathbf{R}) = H^0(\mathbf{r}; \mathbf{R}) + H^{rel}(\mathbf{r}; \mathbf{R}) \quad (1.2)$$

with $H^0(\mathbf{r}; \mathbf{R})$ being the non-relativistic Born-Oppenheimer Hamiltonian

$$H^0(\mathbf{r}; \mathbf{R}) = -\frac{1}{2} \sum_{i=1}^M \nabla_i^2 - \sum_{\alpha,i} \frac{Z_\alpha}{|\mathbf{R}_\alpha - \mathbf{r}_i|} + \frac{1}{2} \sum_{i \neq j}^M \frac{1}{|\mathbf{r}_i - \mathbf{r}_j|} + \frac{1}{2} \sum_{\alpha \neq \beta} \frac{Z_\alpha Z_\beta}{|\mathbf{R}_\alpha - \mathbf{R}_\beta|} \quad (1.3)$$

and $H^{rel}(\mathbf{r}; \mathbf{R})$ encompassing the relativistic contributions (see Ref. 5 and 6). The semi-colon used in the coordinate arguments indicates that the nuclear coordinate is treated as a parameter as opposed to as a dynamical variable in the expression.

The total wave function $\Psi_L^{eN}(\mathbf{r}, \mathbf{R})$ can be expanded in a complete set of electronic states commonly chosen to be the eigenstates of the electronic Hamiltonian, i.e.

$$\Psi_L^{eN}(\mathbf{r}, \mathbf{R}) = \sum_I \Psi_I^0(\mathbf{r}, \mathbf{R}) F_I^L(\mathbf{R}) \quad (1.4)$$

with

$$H^0(\mathbf{r}; \mathbf{R}) \Psi_I^0(\mathbf{r}; \mathbf{R}) = E_I^0(\mathbf{R}) \Psi_I^0(\mathbf{r}; \mathbf{R}) \quad (1.5)$$

Inserting the ansatz for the wave function above into the Schrödinger equation and taking the dot product with the electronic basis states leads to a set of coupled differential equations for the nuclear motion. In the Born-Oppenheimer approximation the interstate couplings are ignored (see Ref. 7) and the nuclear motion is treated independently for each electronic state

$$(T^{nuc} + E_I^0(\mathbf{R})) F_I(\mathbf{R}) = E F_I(\mathbf{R}) \quad (1.6)$$

The electronic energy, which depends on the nuclear coordinates, thus provides a multi-dimensional potential energy surface (PES)⁸ on which the nuclei move. The topology of this surface determines the equilibrium structures of the system through its local and global energy minima and forms the basis for the vibrational motion about such equilibria.

For simplicity we will denote the particular potential energy surface under consideration by

$$V(\mathbf{R}) = E_I^0(\mathbf{R}) \quad (1.7)$$

To begin analyzing the vibrational motion we first Taylor expand this potential about an equilibrium nuclear configuration, noting that the first derivatives are zero at such a point

$$V(\mathbf{R}) = \frac{1}{2} \sum_{i,j} \left(\frac{\partial^2 V}{\partial x_i \partial x_j} \right)_{eq} x_i x_j + \frac{1}{3!} \sum_{i,j,k} \left(\frac{\partial^3 V}{\partial x_i \partial x_j \partial x_k} \right)_{eq} x_i x_j x_k + \mathbf{K} \quad (1.8)$$

where x_i are the nuclear Cartesian coordinates and the indices i, j run over all the coordinates of the N nuclei from 1 to $3N$, following the convention $x_1, y_1, z_1, x_2, y_2, z_2, \dots, x_N, y_N, z_N$.

For small (low energy) oscillations one typically employs the *harmonic* approximation, which consists of truncating the series after the quadratic terms⁹

$$V(\mathbf{R}) = \frac{1}{2} \sum_{i,j} \left(\frac{\partial^2 V}{\partial x_i \partial x_j} \right)_{eq} x_i x_j \quad (1.9)$$

In the framework of the harmonic approximation, fundamental vibrational frequencies of molecules ω_i are obtained by diagonalizing the force constant matrix \mathbf{F}_x , whose elements are simply the second derivatives of the potential

$$\begin{aligned} \boldsymbol{\omega}^2 &= \mathbf{U} \mathbf{M}^{-1/2} \mathbf{F}_x \mathbf{M}^{-1/2} \mathbf{U}^\dagger \\ [\mathbf{F}_x]_{ij} &= \frac{\partial^2 V}{\partial x_i \partial x_j} \quad ; \quad [\mathbf{M}]_{ij} = m_i \delta_{ij} \quad ; \quad [\boldsymbol{\omega}]_{ij} = \omega_i \delta_{ij} \end{aligned} \quad (1.10)$$

where m_i are the nuclear masses. The matrix \mathbf{U} in turn defines the normal mode coordinates via

$$Q_{ir} = \sum_{j=1}^N \sum_{s=1}^3 u(ir)_{js} q_{js} = \sum_{j=1}^N \sum_{s=1}^3 u(ir)_{js} \sqrt{m_j} x_{js} \quad (1.11)$$

and the harmonic vibrational Hamiltonian can be expressed as a sum of harmonic oscillators Hamiltonians

$$H_0 = -\frac{\hbar^2}{2} \sum_{j=1}^N \sum_{s=1}^3 \frac{\partial^2}{\partial Q_{js}^2} + \frac{1}{2} \sum_{j=1}^N \sum_{s=1}^3 k_{js} Q_{js}^2 = \sum_{j=1}^N \sum_{s=1}^3 H_{js} \quad (1.12)$$

The sequence of approximations outlined above give rise to a highly tractable set of equations by which we may find approximate equilibrium structures as well as approximate transition energies.

In the TCU Molecular Physics Laboratory we regularly perform theoretical calculations based on the approximations above in order to aid in the identification of new molecular species.^{10,11} Although the approximate theoretical vibrational frequency can be useful in such identifications, far more greater predictive power can be obtained by employing the method of isotopic substitution in order to provide a more unique “finger print” for a particular system.

In the harmonic approximation it is particularly simple to obtain the *exact* shift in the vibrational frequency resulting from a change in the isotopic masses of a molecule since they are readily obtained from a re-diagonalization of the mass-weighted force constant matrix.^{12,13} Isotopic spectra can thus be readily generated for given isotopic mixes in order to model the result of a specific experiment. In reverse, the isotopic signature obtained in an experiment can also be used in order to deduce geometrical and constitutional properties of the source molecule.

In addition to being of use in identifying new molecular species, the isotopic effect can be used to *probe* a potential in order to provide additional information about the

theoretically obtained potential energy surface. In general, theoretical calculations offer good predictions of isotopic spectra; however, the two approximations that define the harmonic approximation affect the calculation of fundamental vibrational frequencies and isotopic shifts. The inaccuracies related to the calculation of the force constant matrix give rise to errors of the *harmonic* frequencies and the neglect of the higher order terms of the Taylor's series expansion of the nuclear potential introduces errors related to the *anharmonicity* of the actual nuclear potential. These factors give rise to deviations that are reflected in the comparison between theoretical and experimental isotopic spectra, and understanding the details of these deviations can provide clues about the significance of improving specific parts of the theory.

As a result of the above inaccuracies, the vibrational fundamental frequencies calculated in the harmonic approximation are typically higher in frequency than the corresponding experimental measurements. More sophisticated and computationally expensive quantum chemistry methods can provide successively improved values for harmonic frequencies but become increasingly intractable for larger molecules. In addition, anharmonic corrections can be included either through the calculation of an extended potential energy surface on which the nuclear motion can be obtained by various techniques (see Ref. 14 and 15) or by the use of perturbation theory using the higher order derivatives of the Taylor expansion of the potential.^{16,17,18} In essence there is a *harmonic limit* which would be based on the exact knowledge of the leading term of the Taylor expansion as well as an *anharmonic limit* which would include the additional terms exactly. For small systems current methods are close to reaching both these limits but for larger systems one still has to deal with approximate results.

In practice when studying a particular vibrational transition, the theoretically obtained frequency values are scaled by a uniform scaling factor so as to make the frequency one of the isotopomer frequencies in coincidence with the experimental value. Since we in the TCU FTIR laboratory predominantly study carbon cluster this typically means scaling the theoretical value to the isotopomer with all ^{12}C isotopes.

For such a scaling procedure to be accurate two conditions must be fulfilled: *i*) that the harmonic approximation is valid and *ii*) that the error in the force constant can be corrected by scaling each matrix element by the same constant, α^2 . Under these conditions we have that the scaled frequencies are obtained from

$$\boldsymbol{\omega}_{scaled}^2 = \alpha^2 \boldsymbol{\omega}^2 = \mathbf{U} \mathbf{M}^{-1/2} \alpha^2 \mathbf{F}_x \mathbf{M}^{-1/2} \mathbf{U}^\dagger \quad (1.13)$$

Both of these conditions can be more or less accurate depending on the system. In practice one finds that *i*) different theoretical harmonic frequencies scale by different scaling factors and that *ii*) anharmonic effects are mass dependent and that all isotopomers therefore do not scale in the exact same way.

In our group, the application of perturbation theory in the study of isotopically shifted frequencies has offered a better understanding of the behavior of the molecular vibrational frequencies upon isotopic substitutions. By treating isotopic substitutions as mass perturbations, analytical finite order expressions for first and second order contributions to isotopic shifts have allowed us to more fully understand and predict when the traditional method of calculating isotopic frequencies breaks down. In fact, even though isotopic shifts can be calculated exactly in the harmonic approximation, we find that the shifted frequencies for molecules having near-lying vibrational fundamentals may be highly sensitive to the details of the harmonic force constant matrix.

By analyzing the isotopic shifts to second order in perturbation theory, symmetry-allowed interactions or couplings between vibrational modes of a molecule may for example arise as a result of an isotopic substitution (see ref. 19). A typical second order expression in Rayleigh-Schrödinger perturbation theory (RSPT)

$$E_n^{(2)} = \sum_{p \neq n} \sum_i \frac{|\langle \phi_p^i | W | \phi_n \rangle|^2}{E_n^0 - E_p^0} \quad (1.14)$$

where E_n^0 is the unperturbed energy of a state $|\phi_n\rangle$ and W represents a perturbation shows that a large shift in energy, and therefore in transition frequency, can result if the matrix element in the numerator is non-zero and the denominator becomes small. Thus, something that in a first approximation would seem to be a property of a particular vibrational mode, i.e. how it responds to a change in mass, becomes something that depends on more *global* properties of the potential energy surface. Similarly, by analyzing the anharmonic response of the system to a change in mass one can gain insights into how important such effects are for the system. In addition, when anharmonic theoretical calculations are feasible and anharmonic information can be extracted from experiment, such information can be used to aid in the identification of new molecular species.

In the TCU Molecular Physics Laboratory FTIR experiments together with concomitant theoretical modeling of molecular structures and spectra has been a highly successful approach in identifying new molecular species.^{20,21,22,23,24,25} In particular, the method of isotopic substitution has proved to be a key approach in such identifications. Of particular interest in this work are the isotopic spectra of pure carbon clusters, both linear^{26,27,28,29,30,31} and cyclic.^{32,33} Such clusters have been the topic of intense study due to

their relevance in the broader picture of carbon chemistry,^{34,35,36} including the formation of fullerenes.^{37,38}

The number of vibrational fundamentals increases for a linear molecule with N atoms as $3N - 5$ (see Ref. 31). Out of these, $N - 1$ are stretching modes and the remaining $2N - 4$ are bending modes ($N - 2$ if one consider that they are doubly degenerate). The infrared transition probability for the excitation of a stretching fundamental is typically several orders of magnitude larger than for bending modes making stretching modes much more accessible to spectroscopic analysis. By considering a linear vibrating mass model system one can also show that such systems exhibit a maximum fundamental frequency.³⁹ Together with the fact that the number of fundamentals increases with the number of atoms, the density of vibrational fundamentals increases with chain length. As a result, the probability of longer carbon chains having several fundamentals close in frequency increases. Lately, this has proven to be a challenge to the application of the method of isotopic substitution to longer carbon chains.⁴⁰ As discussed above, such situations lead to uncertainties in the predicted isotopic spectral pattern due to the possibility of interactions between several vibrational fundamentals. Cárdenas recently presented assignments to a number of new linear carbon chains based on work in the TCU Molecular Physics Laboratory (see Ref. 40). Many of these assignments and identifications were tentative due to the fact that the theoretical predictions could be shown to have large uncertainties, augmented by the fact that the experimental spectra included contributions from a large number of clusters with overlapping isotopic spectra.

In addition to the issues of the level of accuracy of the calculated harmonic isotopic spectrum one also has to consider the relevance of anharmonic corrections. In practice such

corrections have typically been ignored and expected to be more or less made irrelevant when studying isotopic spectra by the scaling procedure described above. However, anharmonic effects are readily observable in our spectra and in cases with complicated and overlapping spectra, taking anharmonicity into account may show to be important.

In brief, the main goal of the present work has been to investigate two main theoretical issues related to the calculation of isotopic shift spectra:

- Sensitivity of simulated isotopic spectra due to the interactions of vibrational fundamentals
- Sensitivity of simulated isotopic spectra due to the anharmonicity of the interaction potential.

From the investigation of these issues, two theoretical methods were developed as an attempt to aid in the interpretation of experimental isotopic spectra of homonuclear molecules.

Thus, the present work has been structured as follows: Chapter II presents the theoretical framework of how this work was developed. Chapter III addresses the sensitivity of simulated isotopic spectra that is produced by the interactions of vibrational fundamentals. This chapter also introduces an approach for the interpretation of isotopic spectra, called *the isotopic deperturbation method*, which was designed to aid dealing with the aforementioned sensitivity. The applicability of this method is demonstrated on the isotopic spectra of linear C_n ($n= 3, 12$). Chapter IV addresses the effects of anharmonicity on isotopic spectra of homonuclear molecules. Also, this chapter introduces a method to estimate the anharmonicity of vibrational fundamentals from isotopic shift measurements, which arose from our attempt to understand the effects of anharmonicity on isotopic shifts.

The applicability of this method is illustrated on experimental isotopic shift measurements of carbon clusters. Finally, Chapter V presents the conclusions and future work of this investigation.

CHAPTER II. THEORETICAL FRAMEWORK

As noted earlier, the *Born-Oppenheimer Approximation* and the *Harmonic Approximation* are typically employed in the description of the nuclear motion in a molecule in order to make the problem more tractable.

The Born-Oppenheimer approximation^{2,4,5} consists of the separation of the electronic and nuclear motions as a consequence of the small mass ratio between electrons and nuclei. In this approximation the electrons' motion is assumed to take place in a field with *fixed* nuclei since the nuclei's motion is considerably slower than the electrons' motion.² This assumption allows one to calculate the variations of the energy in a molecular system for different fixed-nuclei-configurations, generating the *Potential Energy Surface* (PES) on which the nuclear motion takes place (see Ref. 8).

While considering motion near potential minima we furthermore approximate the PES to the first (non-zero) term in its Taylor expansion, giving rise to the *Harmonic Approximation*.

2.1. The Harmonic Approximation

As mentioned, the harmonic approximation for small oscillations in nuclear vibrational motion consists of expanding the PES in Taylor's series about a local minimum point, (*i.e.*, about an equilibrium position of the nuclei), and truncating the expansion after the quadratic term.⁹

In this expansion, the potential at the local minimum is chosen for convenience to be zero, and the first derivatives of the potential with respect to the nuclear Cartesian coordinates vanish since they are evaluated about a critical point. Thus, for this approximation, the quadratic terms are the only remaining terms in the expansion, leading to a vibrational Hamiltonian

$$H_0 = -\sum_{i=1}^N \frac{1}{2m_i} \nabla_i^2 + \frac{1}{2} \sum_{i=1}^{3N} \sum_{j=1}^{3N} f_{ij} x_i x_j \quad (2.1)$$

The first term in Eq. (2.1) represents the sum of the kinetic energies of the N nuclei, and f_{ij} in the second term represent the second derivatives of the potential with respect to the coordinates x_i . Here the indices i, j run over all the coordinates of the N nuclei from 1 to $3N$, following the convention $x_1, y_1, z_1, x_2, y_2, z_2, \dots, x_N, y_N, z_N$. We reiterate that relativistic effects as well as mass-polarization and coupling terms appearing in the separation of the nuclear and electronic motion⁷ have been neglected in this Hamiltonian.

The relevance of truncating the expansion of the PES rests upon the introduction of a new set of coordinates, named normal coordinates Q_j , which are formed by linear combinations of the nuclei Cartesian coordinates. This set of coordinates allows the transformation of the Hamiltonian (2.1) into a set of independent harmonic oscillator Hamiltonians (see Appendix A for details)

$$H_0 = -\frac{1}{2} \sum_{j=1}^{3N} \frac{\partial^2}{\partial Q_j^2} + \frac{1}{2} \sum_{j=1}^{3N} k_j Q_j^2 = \sum_{j=1}^{3N} H_j \quad (2.2)$$

From a classical point of view the motions described by the normal coordinates Q_j represent the *normal modes of vibration* of a molecule, that is, the set of fundamental motions whose linear superposition describes the actual vibration of the molecule.

2.1.1. Vibrational Frequencies and the “Exact” Calculation of Isotopic Shifts

The introduction of normal coordinates reduces the problem of finding the fundamental frequencies of the normal modes of vibration to an algebraic problem consisting of the diagonalization of the mass-weighted Cartesian Hessian matrix (see Appendix A)

$$\mathbf{M}^{-1/2}\mathbf{F}_x\mathbf{M}^{-1/2} \quad (2.3)$$

Here, the matrix elements of the Cartesian Hessian matrix \mathbf{F}_x correspond to the second derivatives of the PES with respect to the nuclear Cartesian coordinates

$$[\mathbf{F}_x]_{ij} = f_{ij} = \frac{\partial^2 V}{\partial x_i \partial x_j} \quad (2.4)$$

and the matrix $\mathbf{M}^{-1/2}$ is formed with the reciprocal of the square root of the atomic masses on its diagonal.

Thus, fundamental vibrational frequencies are given by

$$\boldsymbol{\omega}_{(0)}^2 = \mathbf{U}_{(0)}\mathbf{M}^{-1/2}\mathbf{F}_x\mathbf{M}^{-1/2}\mathbf{U}_{(0)}^\dagger \quad (2.5)$$

where $\boldsymbol{\omega}_{(0)}^2$ is a diagonal matrix whose elements are the square of the vibrational frequencies $\omega_{(0)}$. $\mathbf{U}_{(0)}$ represents the matrix that diagonalizes $\mathbf{M}^{-1/2}\mathbf{F}_x\mathbf{M}^{-1/2}$, with its columns containing the vibrational modes of the molecule. For convenience, the subscript (0) is used to distinguish from the case that follows.

The vibrational fundamentals of a molecule experience a frequency shift when isotopic substitutions in one or more atoms of the molecule occur; these frequency shifts are referred to as isotopic shifts. In the framework of the harmonic approximation, the *exact* calculation of isotopic shifts consists of changing the masses in the matrix elements

of \mathbf{M} that correspond to the specific substituted atoms, leading to a matrix \mathbf{M}' , and repeating a diagonalization process

$$\boldsymbol{\omega}^2 = \mathbf{U}\mathbf{M}'^{-1/2}\mathbf{F}_x\mathbf{M}'^{-1/2}\mathbf{U}^\dagger \quad (2.6)$$

It is worth noting that the same Cartesian force-constant matrix \mathbf{F}_x is used to calculate the isotopically shifted frequencies because the electronic motion in the Born-Oppenheimer approximation is decoupled from the vibrational motion, and does not depend on the nuclear masses.

2.2. Rayleigh-Schrödinger Perturbation Theory

Perturbation theory plays a fundamental role in our investigation of the effects produced by isotopic substitutions, and the anharmonic nature of the PES on the vibrational frequencies of a molecule.

In the framework of quantum mechanics, physical conservative systems are studied by means of solving the eigenvalue equation of the Hamiltonian operator.⁴¹ However, only a limited number of physical systems are simple enough to have an exact analytical solution of the eigenvalue equation.

Perturbation theory is an approximation method that makes it possible to obtain approximated analytical solutions for some of the physical systems that can not be solved exactly. The applicability of perturbation theory is confined to physical systems whose Hamiltonian H can be expressed as

$$H = H_0 + W \quad (2.7)$$

where the operator H_0 represents the Hamiltonian of a system whose eigenvalues E_n^0 and eigenvectors $|\varphi_n\rangle$ are known. W represents a *small* correction to the Hamiltonian,

containing “less significant” effects of the physical system, which were initially neglected in H_0 . The operator H_0 is called the “unperturbed Hamiltonian” and W is called the “perturbation”. For conservative systems these operators are time-independent, and the approximation method is thus called stationary perturbation theory.

The perturbation W is assumed to be proportional to a real-dimensionless parameter λ , which is smaller than 1 and characterizes the intensity of the perturbation

$$W = \lambda \hat{W} \quad (2.8)$$

$$\lambda \ll 1$$

The Hamiltonian (2.7) is thus written as

$$H(\lambda) = H_0 + \lambda \hat{W} \quad (2.9)$$

where the unperturbed Hamiltonian obeys the eigenvalue equation

$$H_0 |\varphi_n\rangle = E_n^0 |\varphi_n\rangle \quad (2.10)$$

and $H(\lambda)$ obeys the equation

$$H(\lambda) |\psi(\lambda)\rangle = E(\lambda) |\psi(\lambda)\rangle \quad (2.11)$$

The approach followed by perturbation theory to find the modifications introduced by the perturbation is based on the expansion of the eigenvalues and eigenvectors of $H(\lambda)$ in powers of λ

$$E(\lambda) = \varepsilon_0 + \lambda \varepsilon_1 + \dots + \lambda^q \varepsilon_q + \dots \quad (2.12)$$

$$|\psi(\lambda)\rangle = |0\rangle + \lambda |1\rangle + \dots + \lambda^q |q\rangle + \dots \quad (2.13)$$

The coefficients of expansion ε_q and vectors $|q\rangle$ are found by substituting Eqs. (2.9), (2.12) and (2.13) in Eq. (2.11), and equating the coefficients of successive orders of λ on

both sides (see Ref. 41). The use of Eq. (2.10) and the normalization condition for $|\psi(\lambda)\rangle$ is also required for this process.

In the case of a non-degenerate eigenvalue E_n^0 of the unperturbed Hamiltonian H_0 , associated with the eigenstate $|\varphi_n\rangle$, the analytical expressions for the perturbation theory expansions of the energy and stationary state, corrected to second order in λ by the introduction of a perturbation W , are given by

$$E_n(\lambda) = E_n^0 + \langle \varphi_n | W | \varphi_n \rangle + \sum_{p \neq n} \frac{|\langle \varphi_p | W | \varphi_n \rangle|^2}{E_n^0 - E_p^0} + \dots \quad (2.14)$$

$$\begin{aligned} |\psi_n(\lambda)\rangle = & |\varphi_n\rangle + \sum_{p \neq n} \frac{\langle \varphi_p | W | \varphi_n \rangle}{E_n^0 - E_p^0} |\varphi_p\rangle + \sum_{p \neq n} \sum_{l \neq n} \frac{\langle \varphi_l | W | \varphi_p \rangle \langle \varphi_p | W | \varphi_n \rangle}{(E_l^0 - E_p^0)(E_n^0 - E_p^0)} |\varphi_l\rangle \\ & - \langle \varphi_n | W | \varphi_n \rangle \sum_{l \neq n} \frac{\langle \varphi_l | W | \varphi_n \rangle}{(E_n^0 - E_l^0)^2} |\varphi_l\rangle + \dots \end{aligned} \quad (2.15)$$

In practice, when perturbation theory is used for studying a physical system, the terms shown in the energy expansion in Eq. (2.14) are typically the most significant terms. This approximation method is originally applied under the assumption that the perturbation W is small,* therefore, a *fast* convergence of the series is expected. These terms are referred to as the 0th, 1st and 2nd-order corrections, respectively

* The perturbation W is considered to be small when its matrix elements are much smaller than the differences between the eigenvalues of H_0 .

$$\begin{aligned}
E_n^{(0)} &= E_n^0 \\
E_n^{(1)} &= \langle \varphi_n | W | \varphi_n \rangle \\
E_n^{(2)} &= \sum_{p \neq n} \frac{|\langle \varphi_p | W | \varphi_n \rangle|^2}{E_n^0 - E_p^0}
\end{aligned} \tag{2.16}$$

The Eqs. (2.16) have been used in the present work to derive analytical expressions for the first- and second-order corrections to the harmonic vibrational frequencies of a molecule, when isotopic substitutions and anharmonic effects are treated as perturbations.

2.3. Occupation Number Representation

The derivations regarding the perturbation theory treatment of isotopic substitutions and anharmonic effects that are presented in this work have been developed in the *occupation number representation*.

As mentioned in Section 2.1, the Hamiltonian describing molecular vibrations in the harmonic approximation corresponds to a set of independent harmonic oscillator Hamiltonians [see Eq. (2.2)]. The simplest and most common approach to obtaining the quantum spectrum of a set of harmonic oscillator Hamiltonians is by solving its eigenvalue equation in the *occupation number representation* $\{|n\rangle\}$.⁴² In this representation the states of the vibrational Hamiltonian (2.2) are considered as the states of a system consisting of many quasi-particles (phonons), where each of these states is filled with a certain number of identical quasi-particles. Thus, a state $|n_r\rangle$ in the number representation contains n phonons with the same energy, $\hbar\omega_r$.

The occupation number representation arises from the introduction of two operators, a_r and a_r^\dagger , defined as a linear combination of the generalized coordinates \hat{Q}_r and momenta \hat{P}_r (with $\hbar = 1$ and the mass $m = 1$)

$$\begin{aligned} a_r &= \sqrt{\frac{\omega_r}{2}} \left(\hat{Q}_r + \frac{i}{\omega_r} \hat{P}_r \right) \\ a_r^\dagger &= \sqrt{\frac{\omega_r}{2}} \left(\hat{Q}_r - \frac{i}{\omega_r} \hat{P}_r \right) \end{aligned} \quad (2.17)$$

Based on the form in which these operators act on the states $|n_r\rangle$, a_r and a_r^\dagger are interpreted as operators annihilating and creating a particle in the many-phonon system with states $|n_r\rangle$

$$\begin{aligned} a_r^\dagger |n_r\rangle &= \sqrt{n_r + 1} |n_r + 1\rangle \\ a_r |n_r\rangle &= \sqrt{n_r} |n_r - 1\rangle \end{aligned} \quad (2.18)$$

The operators (2.17) satisfy the commutation relations

$$\begin{aligned} [a_r, a_s^\dagger] &= \delta_{r,s} \\ [a_r, a_s] &= [a_r^\dagger, a_s^\dagger] = 0 \end{aligned} \quad (2.19)$$

and any state $|n_r\rangle$ can be expressed in terms of the ground state of the system, this is, when $n_r = 0$ for all n_r , by means of the following recurrence relation

$$|n_r\rangle = \frac{1}{\sqrt{n_r!}} (a_r^\dagger)^{n_r} |0\rangle \quad (2.20)$$

The vibrational Hamiltonian (2.2) is written in the occupation number representation by solving for the operators \hat{Q}_r and \hat{P}_r from Eq. (2.17)

$$\begin{aligned}\hat{Q}_r &= \sqrt{\frac{1}{2\omega_r}} (a_r^\dagger + a_r) \\ \hat{P}_r &= i\sqrt{\frac{\omega_r}{2}} (a_r^\dagger - a_r)\end{aligned}\tag{2.21}$$

and making use of the commutation relations (2.19) (see Ref. 42). Thus, the vibrational Hamiltonian in the occupation number representation takes the form

$$H_0 = \sum_{r=1}^M \omega_r \left(a_r^\dagger a_r + \frac{1}{2} \right)\tag{2.22}$$

The eigenvalues of the Hamiltonian (2.22) are given by

$$E_n = \sum_{r=1}^M \omega_r \left(n_r + \frac{1}{2} \right)\tag{2.23}$$

where $n_r = 0, 1, 2, 3, \dots$. Writing the vibrational ground state energy as ($n_r = 0$ for all n_r)

$$E_0 = \frac{1}{2} \sum_{r=1}^M \omega_r\tag{2.24}$$

the eigenvalues given by Eq. (2.23) can be written as

$$E_n = E_0 + \sum_{r=1}^M \omega_r n_r\tag{2.25}$$

This expression supports what was mentioned earlier in this section; an excited vibrational state of a molecule is equivalent to a system of quasi-particles, with n_r quasi-particles in the state r and frequency ω_r .

In order to develop a perturbation theory treatment of isotopic substitutions and anharmonic effects in the number representation, the Eqs. (2.21) are used to express the respective perturbations in terms of the creation and annihilation operators. The Eqs. (2.18) through (2.20) are applied during the evaluation of the matrix elements of these

perturbations, which appear in the expressions for the corrections to different orders in perturbation theory.

2.4. Isotopic Substitution as a Mass Perturbation

As mentioned earlier, isotopically shifted frequencies can be calculated exactly using the procedure described in Section 2.1.1. However, in addition to the exact calculation given by Eq. (2.6), we have found value in studying the effects of isotopic substitution using perturbation theory by considering an isotopic mass substitution as an *isotopic mass perturbation*. The matrix multiplication on Eq. (2.6) does not offer a simple view of how the normal modes contained in the matrix \mathbf{U} contribute to the frequency shifts. In contrast, the application of perturbation theory has allowed us to obtain analytical finite order expressions for isotopically shifted frequencies, providing a better understanding of the behavior of the molecular vibrational frequencies upon isotopic substitutions.

For the perturbation theory treatment, the Hamiltonian describing the nuclear motion in the harmonic approximation plays the role of the unperturbed Hamiltonian H_0 for a specific set of nuclear masses $\{m_i\}$

$$H_0 = -\frac{1}{2} \sum_{j=1}^{3N} \frac{\partial^2}{\partial Q_j^2} + \frac{1}{2} \sum_{j=1}^{3N} k_j Q_j^2 \quad (2.26)$$

Note that the mass dependence in Eq. (2.26) is implicit in the normal mode coordinates Q_j , which depend on the mass-weighted Cartesian coordinates (see Appendix A).

A substitution of the n th nuclear mass $m_n(i)$ of a molecule, by an isotope with mass $m_n(f)$, produces a difference in the nuclear kinetic energy that can be added in the form of the following perturbation to the unperturbed Hamiltonian (2.1):

$$W_n(i \rightarrow f) = \frac{1}{2m_n(i)} \nabla_n^2 - \frac{1}{2m_n(f)} \nabla_n^2 \quad (2.27)$$

where i and f stand for initial and final mass, respectively. Multiple isotopic substitutions on K atoms of a molecule are described by the sum of single isotopic mass perturbations

$$W_{iso} = \sum_{n=1}^K W_n(i \rightarrow f) = \sum_{n=1}^K \left(\frac{1}{2m_n(i)} \nabla_n^2 - \frac{1}{2m_n(f)} \nabla_n^2 \right) \quad (2.28)$$

The perturbed Hamiltonian is thus written as:

$$H = H_0 + W_{iso} \quad (2.29)$$

In order to simplify later derivations, the mass perturbation [Eq. (2.28)] is written in the number representation, in which the wave functions are mass independent; all mass dependence is contained in the mass perturbation when Eq. (2.28) is expressed in terms of the ladder operators (see Appendix B). As mentioned earlier, the unperturbed Hamiltonian in the number representation has the form

$$H_0 = \sum_{r=1}^M \omega_r \left(a_r^\dagger a_r + \frac{1}{2} \right) \quad (2.30)$$

Also, the isotopic mass perturbation in the number representation takes the form (see Appendix B):

$$W_{iso} [K] = \sum_{rs=1}^M \sum_{n=1}^K \frac{\sqrt{\omega_r^{(0)}} \sqrt{\omega_s^{(0)}}}{4} \left(1 - \frac{m_n(i)}{m_n(f)} \right) \bar{u}_n(r) \bar{u}_n(s) (a_r^\dagger - a_r)(a_s^\dagger - a_s) \quad (2.31)$$

where $\omega_r^{(0)}$ represents the fundamental vibrational frequency associated with the normal mode coordinate Q_r . The vectors $\bar{u}_n(r)$ are the vectors containing the mass-weighted Cartesian coordinates describing the motion of an individual atom in normal mode r .

It is important to note that the mass ratio of the initial and final isotopic masses, as well as the vibrational fundamentals $\omega_r^{(0)}$, play a determinant role in modulating “the strength” of the perturbation given by Eq. (2.31). In general, these factors will determine the overall convergence rate of the series in the perturbation expansion.

In the following sections the isotopic perturbation (2.31), will be used to calculate the first- and second-order corrections to an isotopic shift.

2.4.1. First Order Treatment

It has been stated in Section 2.2 that the first order correction to the energy associated with a state $|\varphi_t\rangle$ in non-degenerate perturbation theory is given by

$$E_t^{(1)} = \langle \varphi_t | W | \varphi_t \rangle \quad (2.32)$$

Experimentally, a fundamental absorption is measured when a transition from the ground state to a single excited vibrational state occurs. Therefore, the first order correction to the frequency shift of a vibrational fundamental, $\omega_t^{(0)}$, produced by the isotopic mass perturbation [Eq. (2.31)], is given by ($\hbar = 1$)

$$\Delta\omega_t^{(1)}[K] = \langle \varphi_t | W_{iso}[K] | \varphi_t \rangle - \langle 0 | W_{iso}[K] | 0 \rangle \quad (2.33)$$

where $|\varphi_t\rangle$ represents a single excited vibrational state. Showing the derivation in Appendix C, Eq. (2.33) takes the form

$$\Delta\omega_t^{(1)}[K] = -\frac{\omega_t^{(0)}}{2} \sum_{n=1}^K \left(1 - \frac{m_n(i)}{m_n(f)}\right) |\vec{u}_n(t)|^2 \quad (2.34)$$

The first order correction in a perturbation theory expansion represents the most predominant term. Equation (2.34) shows that for a given vibrational fundamental, an isotopic shift is mainly determined by the square of the mass-weighted normal mode vector $\vec{u}_n(t)$ of the substituted nucleus. Thus, the isotopic spectrum of a given vibrational mode of a molecule can be roughly predicted to first order by simple inspection of the nuclear normal displacements of that specific mode.

As it will be discussed later, the present work is focused on the study of isotopic shifts associated with single isotopic substitutions. Therefore, the first order correction (2.34) for the particular case of a single isotopic substitution ($K = 1$) simplifies to

$$\Delta\omega_t^{(1)}[n] = -\frac{\omega_t^{(0)}}{2} \left(1 - \frac{m_n(i)}{m_n(f)}\right) |\vec{u}_n(t)|^2 \quad (2.35)$$

2.4.2. Second Order Treatment

The second order correction to the energy in non-degenerate perturbation theory is given by

$$E_t^{(2)} = \sum_{u \neq t} \frac{|\langle \varphi_u | W | \varphi_t \rangle|^2}{E_t^0 - E_u^0} \quad (2.36)$$

For a fundamental vibrational frequency, the second order contribution to the frequency shift of a transition from the ground state to a single excited vibrational state, t , produced by the isotopic mass perturbation [Eq. (2.31)] is given by ($\hbar = 1$)

$$\Delta\omega_t^{(2)}[K] = \omega_t^{(2)}[K] - \omega_0^{(2)}[K] \quad (2.37)$$

The analytical expression of the second order correction takes the form (see appendix D)

$$\Delta\omega_t^{(2)}[K] = 4 \sum_{u \neq t} \frac{\left| \sum_{n=1}^K \frac{\sqrt{\omega_t} \sqrt{\omega_u}}{4} \left(1 - \frac{m_n(i)}{m_n(f)} \right) \bar{u}_n(t) \bar{u}_n(u) \right|^2}{\omega_t - \omega_u} \quad (2.38)$$

$$-4 \sum_u \frac{\left| \sum_{n=1}^K \frac{\sqrt{\omega_t} \sqrt{\omega_u}}{4} \left(1 - \frac{m_n(i)}{m_n(f)} \right) \bar{u}_n(t) \bar{u}_n(u) \right|^2}{\omega_t + \omega_u}$$

Again, considering the particular case of single isotopic substitutions ($K = 1$), the second order contribution to an isotopic shift is given by

$$\Delta\omega_t^{(2)}[n] = 4 \sum_{u \neq t} \frac{\left| \frac{\sqrt{\omega_t^{(0)}} \sqrt{\omega_u^{(0)}}}{4} \left(1 - \frac{m_n(i)}{m_n(f)} \right) \bar{u}_n(t) \bar{u}_n(u) \right|^2}{\omega_t^{(0)} - \omega_u^{(0)}} \quad (2.39)$$

$$-4 \sum_u \frac{\left| \frac{\sqrt{\omega_t^{(0)}} \sqrt{\omega_u^{(0)}}}{4} \left(1 - \frac{m_n(i)}{m_n(f)} \right) \bar{u}_n(t) \bar{u}_n(u) \right|^2}{\omega_t^{(0)} + \omega_u^{(0)}}$$

In general, the calculation of an isotopically shifted frequency to second order in perturbation theory represents a good approximation. But, most important, the analytical expression of the second order correction [Eq. (2.39)] allows us to understand the dependence of an isotopically shifted frequency on the frequencies and nuclear normal mode displacements of *other* vibrational modes; those vibrational modes whose nuclear displacements are *not* orthogonal to the nuclear displacement of the normal mode under study.

In essence, the first and second terms in Eq. (2.39) depend on the same variables, however, the denominators make these terms different. The first term may take a large magnitude when a small denominator results for vibrational fundamentals that are close in

frequency. This term is therefore referred to as the *resonant term*, whereas the second term (the *non-resonant term*) is usually smaller as a consequence of the sum on its denominator. The products of the normal displacements $\bar{u}_n(t)\bar{u}_n(u)$ in Eq. (2.39) give rise to interactions or couplings between vibrational modes upon isotopic substitution, involving the errors of the calculated vibrational fundamentals of other modes in the calculation of the second order corrections of isotopic shifts. The involvement of these errors in the calculations may introduce complications for some cases. These complications and a suggested approach to help dealing with them will be explained in detail in Chapter III.

2.4.3. Self-Shift to Infinite Order

There are some cases where vibrational modes of a molecule remain uncoupled after a particular isotopic substitution. A particular mode, t , remains uncoupled when $\bar{u}_n(r)\bar{u}_n(t) = \delta_{rt}$ for all substituted atoms n . In such a case the isotopic mass perturbation in Eq. (2.31) reduces to

$$\begin{aligned}
 W_{iso} [K] = & \sum_{n=1}^K \frac{\omega_t^{(0)}}{4} \left(1 - \frac{m_n(i)}{m_n(f)} \right) |\bar{u}_n(t)|^2 (a_t^\dagger - a_t)^2 \\
 & + \sum_{rs \neq t}^M \sum_{n=1}^K \frac{\sqrt{\omega_r^{(0)}} \sqrt{\omega_s^{(0)}}}{4} \left(1 - \frac{m_n(i)}{m_n(f)} \right) \bar{u}_n(r) \bar{u}_n(s) (a_r^\dagger - a_r)(a_s^\dagger - a_s)
 \end{aligned} \tag{2.40}$$

It can be shown that for the uncoupled mode, t , the harmonic isotopic frequency is now given to infinite order by

$$\begin{aligned}
 \omega_t' = & \left(1 - \sum_n \lambda_n |\bar{u}_n(t)|^2 \right)^{1/2} \omega_t^{(0)} \\
 \lambda_n = & \left(1 - \frac{m_n(i)}{m_n(f)} \right)
 \end{aligned} \tag{2.41}$$

We refer to the isotopic shift given by Eq. (2.41) as the *self-shift to infinite order* since this frequency shift represents the sum of all the contributions that result from the coupling of the mode t with “itself”.

Furthermore, for a homonuclear system subjected to a uniform shift of all nuclear masses we find that all modes are uncoupled due to the orthogonality of the normal mode coordinates derived from the unitary matrix \mathbf{U} . Thus, Eq. (2.41) reduces to

$$\omega'_t = \left(1 - \lambda \sum_n |\bar{u}_n(t)|^2 \right)^{1/2} \omega_t^{(0)} = \left(\frac{m(i)}{m(f)} \right)^{1/2} \omega_t^{(0)} \quad (2.42)$$

for *all* vibrational modes.

The Eqs. (2.40) and (2.42) will be specially useful in the “*Application and Discussion*” section in Chapter IV.

CHAPTER III. MODE INTERACTION

3.1. Introduction

As mentioned in Section 2.4.2, interactions or couplings between vibrational modes arise in the calculation of isotopic shifts as a consequence of isotopic substitutions. Specifically, the couplings between vibrational modes are caused by the products of mass-weighted normal mode vectors $\vec{u}_n(t)\vec{u}_n(u)$, found in Eq. (2.39). The strength of these couplings is modulated by the aforementioned products and the denominators of each term in Eq. (2.39). In the case of molecules possessing near-lying vibrational fundamentals, the treatment to second order in perturbation theory of isotopically shifted frequencies face problems related to coupling effects. For molecules with near-lying vibrational fundamentals, the contribution of the second order correction to the isotopic shifts may become significant due to a small denominator of the first (resonant) term in Eq. (2.39). The isotopic shift calculation then becomes highly sensitive to the accuracy of the force constant matrix since the errors (originated from all of the approximations assumed) in the calculated vibrational fundamentals and normal mode displacements also become significant in the calculated second order correction.

In addition to the theoretical complications, experimental complications also arise for molecules with near-lying vibrational fundamentals. Experimentally, isotopic spectra of molecules with near-lying vibrational fundamentals exhibit a large number of absorptions in a small region of the spectrum, which significantly complicates its interpretation. The “congestion” in the experimental spectrum, combined with the high sensitivity of the calculations due to the strong interaction between vibrational modes, challenges the

reliability of the band assignment in the comparison of experimental and theoretical isotopic spectra. Thus, the present work introduces an approach, that we call the *isotopic deperturbation method*, designed to aid reducing these complications. This approach allows a comparison between experimental and theoretical isotopic shifts in which the effects of the interactions between vibrational modes (*coupling effects*) that result from second order contributions are not involved. Contrastingly, the approach allows for an additional comparison of the coupling effects exhibited by the experimental and theoretical isotopic shifts, in order to determine whether or not the errors introduced by the interactions between vibrational modes are contributing to the discrepancies between theory and experiment.

3.2. Method

The *isotopic deperturbation method* has been developed to aid in the interpretation of isotopic spectra of non-degenerate vibrational modes of homonuclear molecules ${}^A X_n$, where X represents an element, A the mass number and n the number of atoms.

It is worth noting that this method is applicable to isotopic shifts due to single and multiple isotopic substitutions, however, in the present work only isotopic shifts due to single substitutions have been used in the description and application of this method, for theoretical and experimental reasons. From the perturbation theory perspective, a multiple substitution produces a larger perturbation than a single substitution (see Eq. (2.28)). Therefore, a faster convergence of the perturbation theory expansion will occur with a perturbation due to single substitution, which is convenient for reducing the significance of the higher order terms. Experimentally, an adequate isotopic abundance ratio in the sample can be determined for which the probability of observing absorptions in the spectrum due

to multiple substitutions is lowered substantially. Thus, mainly single isotopic shifts of a vibrational fundamental are detected, reducing the number of absorptions in the spectrum and simplifying its interpretation.

An essential condition for the application of this method is the availability of two complementary isotopic spectra: one with measurements of a vibrational fundamental of all ${}^A X$ species and the isotopic shifts caused by single ${}^B X$ isotopic substitutions; and another one with measurements of a vibrational fundamental of all ${}^B X$ species and the single ${}^A X$ isotopic shifts.

From the point of view of molecular vibrations, ${}^A X_n$ and ${}^B X_n$ species are analogous systems. The isotopic mass perturbation W_A , which is used to calculate isotopic shifts that are produced by single ${}^B X$ substitutions in an otherwise all ${}^A X$ species, is linearly related to the isotopic mass perturbation W_B that is used to calculate isotopic shifts that are produced by single ${}^A X$ substitutions in an otherwise all ${}^B X$ species. It can be noticed from the mass ratio appearing in Eq. (2.31) that the perturbations W_A and W_B are related as

$$W_B = -\frac{1}{\gamma} W_A \quad (3.1)$$

where γ is defined in terms of the isotopic masses, m_A and m_B , of the respective isotopes ${}^A X$ and ${}^B X$

$$\gamma \equiv \sqrt{\frac{m_A}{m_B}} \quad (3.2)$$

The relation given in Eq. (3.1) will be used in the present work to introduce the following approach that allows one eliminating the effects of the second order

contributions from the theoretical and experimental isotopic shifts of the fundamental vibrational frequencies of the ${}^A X_n$ and ${}^B X_n$ species.

An isotopically shifted frequency, ω_A , of an all ${}^A X$ vibrational fundamental, $\omega_A^{(0)}$, can be written in a perturbation theory expansion as

$$\omega_A = \sum_{i=0}^{\infty} \omega_A^{(i)} \quad (3.3)$$

Similarly, an isotopically shifted frequency, ω_B , of an all ${}^B X$ vibrational fundamental, $\omega_B^{(0)}$, can be written as

$$\omega_B = \sum_{i=0}^{\infty} \omega_B^{(i)} \quad (3.4)$$

In the harmonic approximation, the frequency $\omega_A^{(0)}$ of a given vibrational mode of an all ${}^A X$ species is related to the frequency $\omega_B^{(0)}$ of an all ${}^B X$ species by

$$\omega_B^{(0)} = \gamma \omega_A^{(0)} \quad (3.5)$$

Making use of Eq. (3.1), the bracketing theorem (see Appendix E) and Eq. (3.5), the different orders of a shifted frequency ω_B in Eq. (3.4) can be expressed in terms of the orders of the shifted frequency ω_A [Eq. (3.3)] as

$$\omega_B = \gamma \omega_A^{(0)} + \sum_{i=1}^{\infty} \frac{(-1)^i}{\gamma^{2i-1}} \omega_A^{(i)} \quad (3.6)$$

By applying the following “mirror” transformation to Eq. (3.6), a frequency ω_{mirror} can be obtained for the shifted frequency in Eq. (3.6)

$$\omega_{mirror} = \omega_A^{(0)} (1 + \gamma^4) - \gamma^3 \omega_B \quad (3.7)$$

so the second order correction is conveniently adjusted to be equal in magnitude and opposite in sign to its counterpart in Eq. (3.3)

$$\omega_{mirror} = \omega_A^{(0)} + \gamma^2 \omega_A^{(1)} - \omega_A^{(2)} + \sum_{i=3}^{\infty} \frac{(-1)^{i+1}}{\gamma^{2i-4}} \omega_A^{(i)} \quad (3.8)$$

Thus, the second order terms of a pair of isotopically shifted frequencies, ω_A and ω_{mirror} , can be completely eliminated by taking the average between Eq. (3.3) and Eq. (3.8)

$$\omega_{AVG} = \omega_A^{(0)} + \left(\frac{1+\gamma^2}{2}\right) \omega_A^{(1)} + 0 + \left(\frac{1+\frac{1}{\gamma^2}}{2}\right) \omega_A^{(3)} + \left(\frac{1-\frac{1}{\gamma^4}}{2}\right) \omega_A^{(4)} + \left(\frac{1+\frac{1}{\gamma^6}}{2}\right) \omega_A^{(5)} + \dots \quad (3.9)$$

Within the harmonic approximation, Eq. (3.9) allows the entire elimination of the coupling effects related to the second order terms, as well as the suppression of the even order terms. However, a limit for the applicability of this approach arises in Eq. (3.9). The factors multiplying the third and higher order terms in this equation grow significantly as $\gamma \rightarrow 0$, resulting in significant contributions of those terms to ω_{AVG} . At the same time, using Eq. (2.31) and the bracketing theorem one can find that the i th order correction $\omega_A^{(i)}$ depends on γ as

$$\omega_A^{(i)} \propto (1-\gamma^2)^i \quad (3.10)$$

which implies that the convergence of the perturbation theory expansion in Eq. (3.9) can be challenged when $\gamma \ll 1$. Therefore, the approach introduced here to reduce the coupling effects from the comparison between experimental and theoretical isotopic shifts is applicable to cases where

$$\gamma \equiv \sqrt{\frac{m_A}{m_B}} \approx 1 \quad (3.11)$$

A *scaled non-degenerate first order* (SNDFO) shifted frequency ω_A^{SNDFO} is obtained by applying the following scaling factor to an isotopically shifted frequency calculated in non-degenerate first order (NDFO)

$$\omega_A^{SNDFO} = \omega_A^{(0)} + \left(\frac{1 + \gamma^2}{2} \right) \omega_A^{(1)} \quad (3.12)$$

Thus, an SNDFO shifted frequency [Eq. (3.12)] can be compared with an averaged isotopically shifted frequency [Eq. (3.9)]. The coupling effects resulting from second order contributions are not involved in this comparison, which represents the essence of the isotopic deperturbation method.

3.2.1. Application of the Mirror Transformation to Experimental Isotopic Shifts

In the harmonic approximation, the *theoretical* vibrational fundamentals of an all $^A X$ and an all $^B X$ species, $\omega_A^{(0)}$ and $\omega_B^{(0)}$, respectively, are related by Eq. (3.5). However, because of anharmonicity the *experimental* values of these vibrational fundamentals, $\omega_A^{(0),\text{exp}}$ and $\omega_B^{(0),\text{exp}}$, are related by a slightly different scaling factor, γ' , defined as

$$\gamma' = \frac{\omega_B^{(0),\text{exp}}}{\omega_A^{(0),\text{exp}}} \quad (3.13)$$

When working with experimental measurements this small correction has to be taken into account in the perturbation W_B . Therefore, the relation with the perturbation W_A is given by

$$W_B = -\frac{\gamma'}{\gamma} W_A \quad (3.14)$$

Following the same procedure discussed in section 3.2, the *mirror transformation* in Eq. (3.7) is slightly modified to

$$\omega_{mirror} = \omega_A^{(0)} (1 + \gamma^4) - \frac{\gamma^4}{\gamma'} \omega_B \quad (3.15)$$

Thus, the mirrored frequency of an experimental isotopic shift ω_B^{exp} is given by:

$$\omega_{mirrored}^{exp} = \omega_A^{(0),exp} (1 + \gamma^4) - \frac{\gamma^4}{\gamma'} \omega_B^{exp} \quad (3.16)$$

After a mirrored experimental isotopic shift $\omega_{mirrored}^{exp}$ is calculated by Eq. (3.16), the average frequency between $\omega_{mirrored}^{exp}$ and its counterpart ω_A^{exp} is calculated in order to reduce the effects related to the second order terms from the experimental measurements:

$$\omega_{AVG}^{exp} = \frac{\omega_{mirrored}^{exp} + \omega_A^{exp}}{2} \quad (3.17)$$

The partial approach suggested by the isotopic deperturbation method consists of finding the average frequency of a pair of experimental isotopic shifts [using Eq. (3.17)], and comparing it with the corresponding SNDFO isotopic shift. The complete procedure for the application of this method is described next.

3.2.2. Isotopic Deperturbation Method

Provided that harmonic frequencies and the “standard” calculation of isotopic shifts are available (see Section 2.1.1), the application of the isotopic deperturbation method consists of the following steps:

- a) The application of the mirror transformation [Eq. (3.15)] to the *calculated* and *experimental* single isotopic shifts ω_b of the all $^B X$ vibrational fundamental under consideration.

- b) The calculation of the average frequency [Eq. (3.17)] for each pair of experimental isotopic shifts ω_A^{exp} and $\omega_{\text{mirrored}}^{\text{exp}}$.
- c) The calculation to first order in perturbation theory of the single isotopic shifts in question using Eq. (2.35), and scaled by Eq. (3.12), in order to be compared with the average of the experimental isotopic shifts calculated in step (b).

After the application of the procedure described above, the relative positions and spacing among the isotopic shifts produced by a substitution on a particular molecular site can be interpreted by means of Eqs. (2.35) and (2.39).

3.3. Application of Isotopic Deperturbation Method to Linear Carbon Chains

The isotopic deperturbation method has been applied in the interpretation of infrared isotopic spectra of linear C_n ($n = 3 - 12, 15, 18$) (see Ref. 43). Some of these carbon chains ($n \geq 7$) have near-lying vibrational fundamentals and their experimental isotopic spectra exhibit those problems related to the normal mode interaction.

For each of these carbon chains two complementary isotopic spectra were available: one with a vibrational fundamental of the all ^{12}C species and its single ^{13}C isotopic shifts; and its counterpart with the all ^{13}C vibrational fundamental and the single ^{12}C isotopic shifts. The first set of measurements is observed in a low ^{13}C enrichment spectrum, resulting from an experiment in which a 90% ^{12}C : 10% ^{13}C ratio is used. We refer to this spectrum as *90/10 spectrum*. For similar reasons we refer to the later isotopic spectrum as *10/90 spectrum*. As required, the ^{12}C and ^{13}C isotopes satisfy the condition stated in Eq. (3.11)

$$\gamma = \sqrt{\frac{12.00000}{13.00335}} \approx 0.96$$

Harmonic frequencies and normal mode displacements have been calculated with the Gaussian 03⁴⁴ program suite. For all linear C_n ($n = 3 - 12, 15, 18$), the calculation of the force constant matrices were carried out at the same level of theory, DFT/B3LYP with the cc-pVDZ basis set, in order to keep it as a “fixed parameter” since the object of study of the present work is the effects of the interactions originated in the harmonic approximation.

The results obtained after the application of the isotopic deperturbation method to linear C_n ($n = 3 - 12, 15, 18$) can be separated in three groups; the results obtained from: *i*) the already identified⁴⁵ vibrational modes of linear C_n ($n = 3 - 6$), *ii*) the recently assigned⁴⁰ vibrational modes of linear C_n ($n = 7 - 12$), and *iii*) the tentative assignments of the vibrational modes of linear C_n ($n = 15, 18$). These results are presented in the following subsections.

3.3.1. Linear C_n ($n = 3 - 6$)

The isotopic deperturbation method was initially tested by applying it to the interpretation of the isotopic spectra of the already identified vibrational modes of linear C_n ($n = 3 - 6$). Even though these carbon chains have “well separated” vibrational fundamentals and their isotopically shifted frequencies are not expected to experience complications related to strong coupling effects, the application of the method provided beneficial feedback for later applications on longer carbon chains.

The application of the method to the isotopic spectra of the asymmetric stretching mode of linear C_3 is presented in detail as an illustration. Only this representative case will

be discussed in detail since a similar outcome is found, and the same conclusions can be drawn, when the method is applied to the other chains ($n = 4 - 6$).

Linear C₃

Figure 1 shows the application of the isotopic deperturbation method to the isotopic spectra of the $\nu_3(\sigma_u)$ mode of linear C₃.

The following conventions are used on the Figures: labels c1, c2, c3, etc. indicate sets of experimental and predicted isotopic shifts due to a single isotopic substitution on the 1st, 2nd, 3rd, etc. position of a carbon chain, respectively. The *exact spectrum* in blue represents a theoretical simulation that shows the calculated ¹³C isotopic shifts of a vibrational fundamental of an all ¹²C species. The *mirrored spectrum* in red represents a simulation that shows the calculated ¹²C isotopic shifts of a vibrational fundamental of an all ¹³C species after the application of the mirror transformation given by Eq. (3.15). The isotopic shifts simulated in the exact and mirrored spectra correspond to an exact calculation using the method described in section 2.2.1. The *SNDFO spectrum* in green also simulates the ¹³C isotopic shifts of an all ¹²C vibrational fundamental, but these isotopic shifts are calculated to first order in perturbation theory and scaled by Eq. (3.12).

Experimental isotopic shifts are represented by vertical lines (see Figures), obeying the same color convention that is used on the simulations. The blue vertical lines represent experimental ¹³C isotopic shifts. The red vertical lines represent experimental ¹²C isotopic shifts, after applying the mirror transformation given by Eq. (3.16). The green vertical lines represent the average frequencies between the pairs of experimental ¹³C and mirrored-¹²C isotopic shifts, calculated with Eq. (3.17).

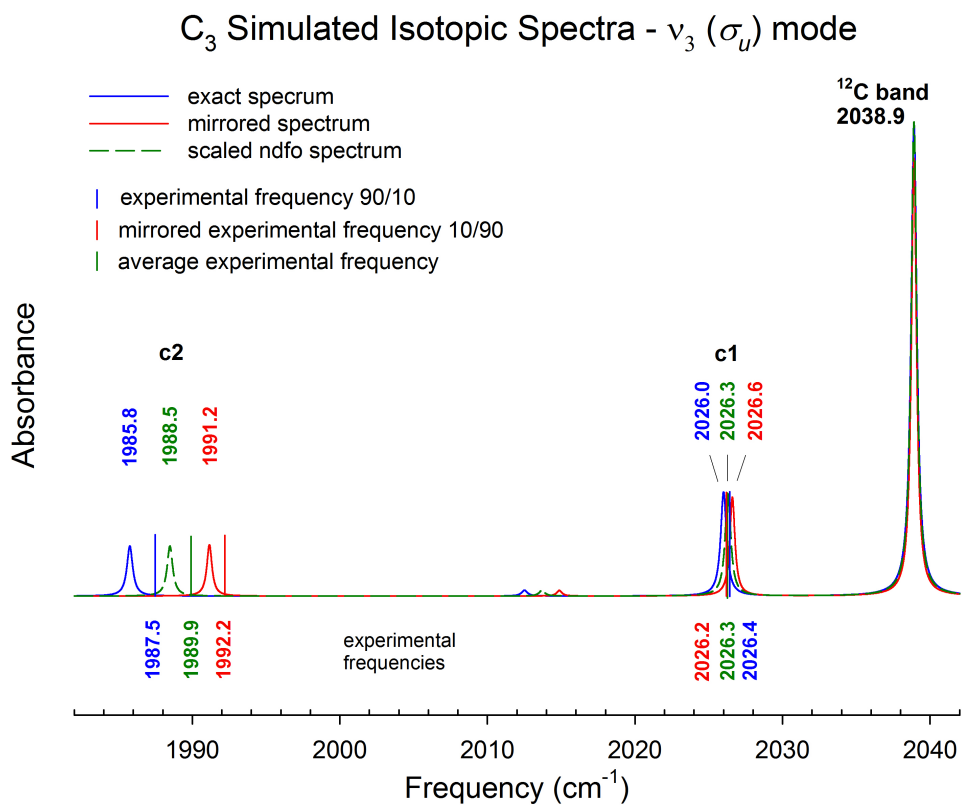


Figure 1. Application of the isotopic deperturbation method to the isotopic spectra of the $\nu_3(\sigma_u)$ mode of linear C₃

Table 1 shows the normal displacements and harmonic frequencies of the stretching modes of linear C₃. It is important to note that the normal mode displacements of the stretching modes of linear C₃ are completely determined by the normalization and fixed-center-of-mass constrains. Therefore, these normal mode displacements of linear C₃ always take the same values, irrespective of the level of theory that is used to calculate the harmonic frequencies.

Stretching Mode	Frequency (cm ⁻¹)	Normal Mode Displacement Vector $\vec{u}_n(t) = (u_1, u_2, u_3)$	
$\omega_1(\sigma_g)$	1241.6519	$\vec{u}_n(1)$	(0.71, 0.00, -0.71)
$\omega_3(\sigma_u)$	2157.8096	$\vec{u}_n(3)$	(-0.41, 0.82, -0.41)

Table 1. Normal mode displacements and harmonic frequencies of the stretching modes of linear C₃, calculated at the DFT/B3LYP level with the cc-pVDZ basis set.

Single isotopic substitutions are possible at positions c1 and c2 for linear C₃; substitutions on positions c1 and c3 are equivalent. A description to first order in perturbation theory with the aid of Eq. (2.35), given by

$$\Delta\omega_i^{(1)}[n] = -\frac{\omega_i^{(0)}}{2} \left(1 - \frac{m_n(i)}{m_n(f)} \right) |\vec{u}_n(t)|^2$$

allows us to understand that an isotopic substitution on position c1, with the smallest normal displacement, produces the smallest isotopic shift [see Table 1, Eq. (2.35) and Figure 1]. In addition to the small normal displacement of this molecular site, there is a large frequency difference between the $\omega_3(\sigma_u)$ and the $\omega_1(\sigma_g)$ vibrational fundamentals, predicted to be about 916 cm⁻¹ (see Table 1). This produces a large denominator in both terms of Eq. (2.39), given by

$$\Delta\omega_t^{(2)} [n] = 4 \sum_{u \neq t} \frac{\left| \frac{\sqrt{\omega_t^{(0)}} \sqrt{\omega_u^{(0)}}}{4} \left(1 - \frac{m_n(i)}{m_n(f)} \right) \bar{u}_n(t) \bar{u}_n(u) \right|^2}{\omega_t^{(0)} - \omega_u^{(0)}}$$

$$- 4 \sum_u \frac{\left| \frac{\sqrt{\omega_t^{(0)}} \sqrt{\omega_u^{(0)}}}{4} \left(1 - \frac{m_n(i)}{m_n(f)} \right) \bar{u}_n(t) \bar{u}_n(u) \right|^2}{\omega_t^{(0)} + \omega_u^{(0)}}$$

resulting in a small second order correction or weak coupling between these normal modes. The spacing and relative positions of a pair of ^{13}C and mirrored- ^{12}C isotopic shifts is referred to as the *coupling effects* since these patterns result from the interaction or coupling between vibrational modes upon isotopic substitution. The small coupling effects are indicated in Figure 1 by the small “separation” between the *harmonic* ^{13}C and mirrored- ^{12}C isotopic shifts, showing good agreement with the respective experimental isotopic shifts.

Qualitatively speaking, the SNDFO isotopic shifts for molecular sites c1 and c2 in Figure 1, determined with Eq. (3.12), are equal to the average frequencies between each pair of *harmonic* ^{13}C and mirrored- ^{12}C isotopic shifts, given by Eq. (3.9). This can be noticed in Figure 1 because the SNDFO isotopic shifts appear in the middle of the frequency interval between the pairs of *harmonic* ^{13}C and mirrored- ^{12}C isotopic shifts. This implies that third and higher orders in Eq. (3.9) are negligible and therefore the treatment to second order in perturbation theory is sufficient.

The isotopic shifts due to isotopic substitution of position c2 illustrate the contribution of the non-resonant term in Eq. (2.39). For this substitution, there is no coupling between the $\omega_3(\sigma_u)$ and $\omega_1(\sigma_g)$ vibrations because the normal displacement of the

central position is zero for the symmetric stretch $\omega_1(\sigma_g)$ (see Table 1). The second order contribution to the isotopic shift results from the second term in Eq. (2.39), the non-resonant term, because this term sums over all normal modes; it includes the coupling of the $\omega_3(\sigma_u)$ vibration with itself. The negative sign of the non-resonant term produces a shift to the low frequency side of the NDFO isotopic shift for both the ^{13}C and ^{12}C *harmonic* isotopic shifts. However, the shift for the *harmonic* ^{12}C isotopic shift appears to be inverted to the higher frequency side of the NDFO isotopic shift because it has been mirrored. The “spacing” between the *harmonic* ^{13}C and the mirrored- ^{12}C isotopic shifts can be interpreted as an effect of the “self-coupling” of this mode (see Figure 1). Again, experimental isotopic shifts exhibit good agreement with the simulations.

Overall, three main qualitative aspects are consistent in the behavior of the experimental and theoretical isotopic shifts (see Figure 1), and we suggest the comparison of these aspects as an aid for the correct assignment of isotopic shifts in future work:

1. The relative positions of each set of *experimental* isotopic shifts are consistent with the relative positions of the *predicted* isotopic shifts.
2. The spacing among the set of experimental isotopic shifts corresponding to a particular substitution is approximately equal to the spacing exhibited by the analogous prediction.
3. The average frequency of a set of experimental isotopic shifts is not always equal to the corresponding SNDFO isotopic shift, but these frequencies are relatively close.

Thus, the inspection of points (1-3) can help determining whether or not the effects of the interaction between vibrational modes are contributing to complicate the interpretation of the spectra.

In addition to the analysis of the isotopic spectra of linear C_3 in terms of coupling effects, which is offered by the isotopic deperturbation method, evidence of anharmonic effects are found in the comparison between the harmonic and experimental isotopic shifts of the central position, c2, shown in blue and red in Figure 1. First of all, the normal displacements of the stretching modes of a tri-atomic molecule are completely determined from the normalization condition and the condition regarding the stationary center of mass. That is, the nuclear normal displacements of these modes are *unique*. Second, there is no coupling between the $\omega_3(\sigma_u)$ vibration and the other vibrational modes for an isotopic substitution on the central position. In other words, this isotopic shift depends *uniquely* on the normal displacement of the central position. Thus, if the vibration were harmonic and if it is assumed that the absorption at 2038.9 cm^{-1} represents the harmonic vibrational fundamental $\nu_3(\sigma_u)$, the theoretical and experimental isotopic shifts should be identical. For this reason, the observed difference in the comparison between the experimental and harmonic isotopic shifts for this substitution is purely a consequence of the anharmonic vibration of the molecule.

It is important to note that the argument regarding the anharmonic effects is only applicable to the isotopic shifts of the central position (c2) of linear C_3 . However, the level of agreement in the comparison of the experimental and theoretical coupling effects is the same for all C_n ($n = 3 - 6$).

3.3.2. *Linear C_n (n = 7 – 12)*

For these carbon chains, the vibrational fundamentals that have been measured in our lab have a common characteristic: they are predicted to have at least another vibrational fundamental which is close in frequency (less than 100 cm⁻¹). As mentioned earlier, this is the scenario in which strong coupling effects on isotopic shifts can occur and where the sensitivity of simulated isotopic spectra can increase.

The application of the method to the isotopic spectra of the $\nu_7(\sigma_u)$ mode of linear C₁₂ is presented as a representative case since similar results were found when the method was applied to the other chains ($n = 7 - 11$).

Linear C₁₂

For convenience, the application of the isotopic deperturbation method to the $\nu_7(\sigma_u)$ mode of linear C₁₂ is presented in different figures (see Figure 2 – Figure 6), showing in most of the cases one set of isotopic shifts in each Figure. Our discussion will be focused on Figure 3 – Figure 6. In Figure 2, no coupling effects occur since no isotopic shifts occur for isotopic substitutions on the first (c1) and second (c2) molecular sites.

C_{12} Simulated Isotopic Spectra - $\nu_7 (\sigma_u)$ mode

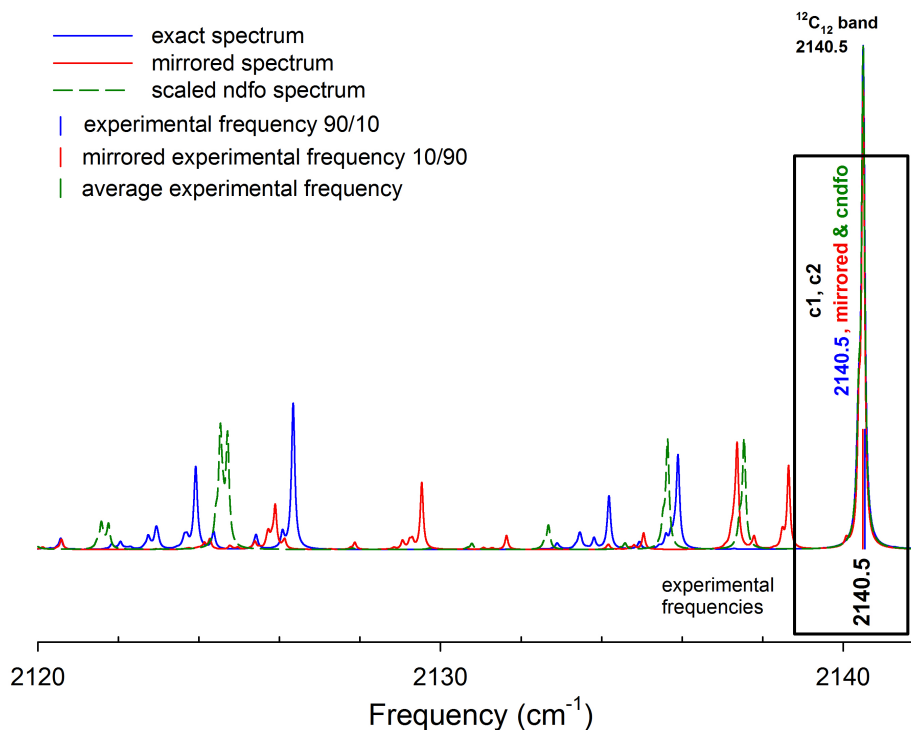


Figure 2. Application of the isotopic deperturbation method to the isotopic spectra of the $\nu_7(\sigma_u)$ mode of linear C_{12} : Isotopic shifts due to substitutions on the first (c1) and second (c2) molecular sites

In Figure 3 – Figure 6 the predicted coupling effects are not in excellent agreement with their experimental counterpart. In each figure the relative positions of a set of simulated isotopic shifts (blue and red spectra) are consistent with the relative positions of the experimental isotopic shifts (blue and red bars), which means that theory is providing a fair approximate description of the interactions between normal modes. However, the spacing exhibited by the pairs of simulated ^{13}C and mirrored- ^{12}C isotopic shifts (blue and red spectra) is not in agreement with the spacing exhibited by the experimental counterparts (blue and red bars), which indicates that the calculations of the second and higher order terms are not entirely accurate.

In this case, the fundamental frequency of the $\nu_7(\sigma_u)$ mode of linear C_{12} is predicted to have two nearby vibrational fundamentals: the $\nu_8(\sigma_u)$ vibrational fundamental $\sim 76 \text{ cm}^{-1}$ lower in frequency, and the $\nu_1(\sigma_g)$ vibrational fundamental $\sim 24 \text{ cm}^{-1}$ higher in frequency. Particularly, the $\nu_1(\sigma_g)$ normal mode is a non-infrared active mode whose actual frequency can not be measured by means of Fourier transform infrared spectroscopy. The actual frequency of the $\nu_1(\sigma_g)$ vibrational fundamental could be found closer or farther to the $\nu_7(\sigma_u)$ vibrational fundamental than the predicted 24 cm^{-1} . Since this uncertainty is involved in the calculation of the second and higher order contributions to the isotopic shifts, and this contributions are significant because $\nu_1(\sigma_g)$ and $\nu_7(\sigma_u)$ are nearby vibrations, the uncertainty also becomes significant. As a result, the predicted coupling effects are affected by this uncertainty and do not exhibit a good agreement with the experimental counterpart (see figures).

In addition to the uncertainty associated with the calculated second order contributions to the isotopic shifts, there are also errors introduced by the first order contributions. These errors are produced by the uncertainty of the calculated normal mode displacements $\bar{u}_n(t)$, which mainly determine the magnitude of the first order corrections [see Eq. (2.35)]. Thus, the errors arising from the calculation of the first order corrections are also contributing to the overall discrepancy between theoretical and experimental isotopic shifts.

C_{12} Simulated Isotopic Spectra - $\nu_7(\sigma_u)$ mode

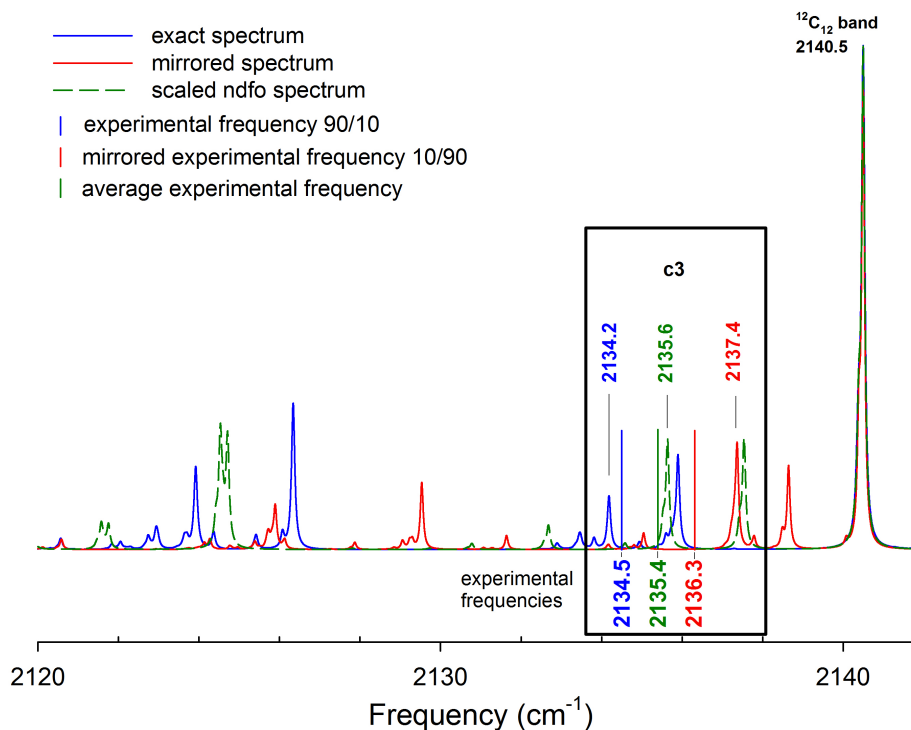


Figure 3. Application of the isotopic deperturbation method to the isotopic spectra of the $\nu_7(\sigma_u)$ mode of linear C_{12} : Isotopic shifts due to substitution on the third (c3) molecular site

Also, it can be observed in Figure 4 that the SNDFO isotopic shift for the c4 substitution (dashed green) is not equal to the average frequency between the pair of *theoretical* ^{13}C and mirrored- ^{12}C isotopic shifts, (the SNDFO isotopic shift is not situated in the middle of the frequency interval between the blue and red simulated isotopic shifts).

From the respective equations used to calculate these frequencies

$$\omega^{SNDFO}(c4) = \omega^{(0)} + \left(\frac{1 + \gamma^2}{2} \right) \omega^{(1)} \quad (3.12)$$

and

$$\omega_{AVG}(c4) = \omega^{(0)} + \left(\frac{1+\gamma^2}{2}\right)\omega^{(1)} + \left(\frac{1+\frac{1}{\gamma^2}}{2}\right)\omega^{(3)} + \left(\frac{1-\frac{1}{\gamma^4}}{2}\right)\omega^{(4)} + \left(\frac{1+\frac{1}{\gamma^6}}{2}\right)\omega^{(5)} + \dots$$

(3.9)

it can be easily noticed that this deviation observed in Figure 4, which corresponds to the difference between the SNDFO isotopic shift ω^{SNDFO} and the average frequency ω_{AVG} , is proportional to the third and higher order contributions to the calculated isotopic shift of the c4 substitution (see Eqs. (3.9) and (3.12)). Thus, the comparison between the SNDFO isotopic shift and the theoretical average frequency allows us to see that the third and higher order terms are significant in this case, and therefore contribute to the predicted coupling effects for this pair of isotopic shifts.

C_{12} Simulated Isotopic Spectra - $\nu_7 (\sigma_u)$ mode

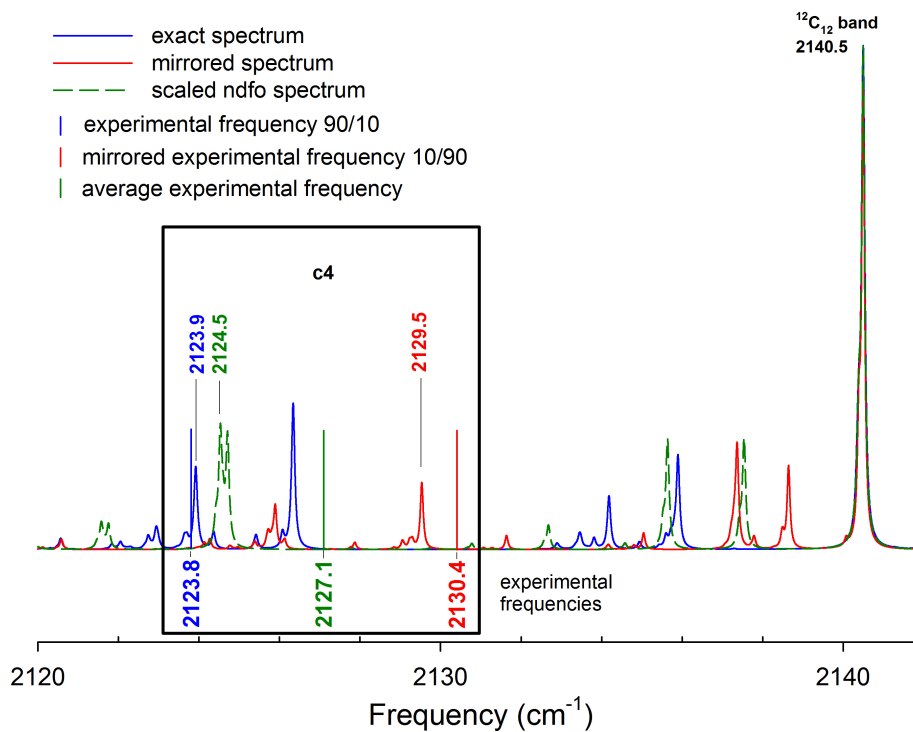


Figure 4. Application of the isotopic deperturbation method to the isotopic spectra of the $\nu_7(\sigma_u)$ mode of linear C_{12} : Isotopic shifts due to substitution on the fourth (c4) molecular site

Figure 5 also shows a scenario in which the third and higher order terms are contributing to the isotopic shift calculation; the SNDFO isotopic shift is not equal to the average frequency between the simulated ^{13}C and mirrored- ^{12}C isotopic shifts.

C_{12} Simulated Isotopic Spectra - $\nu_7 (\sigma_u)$ mode

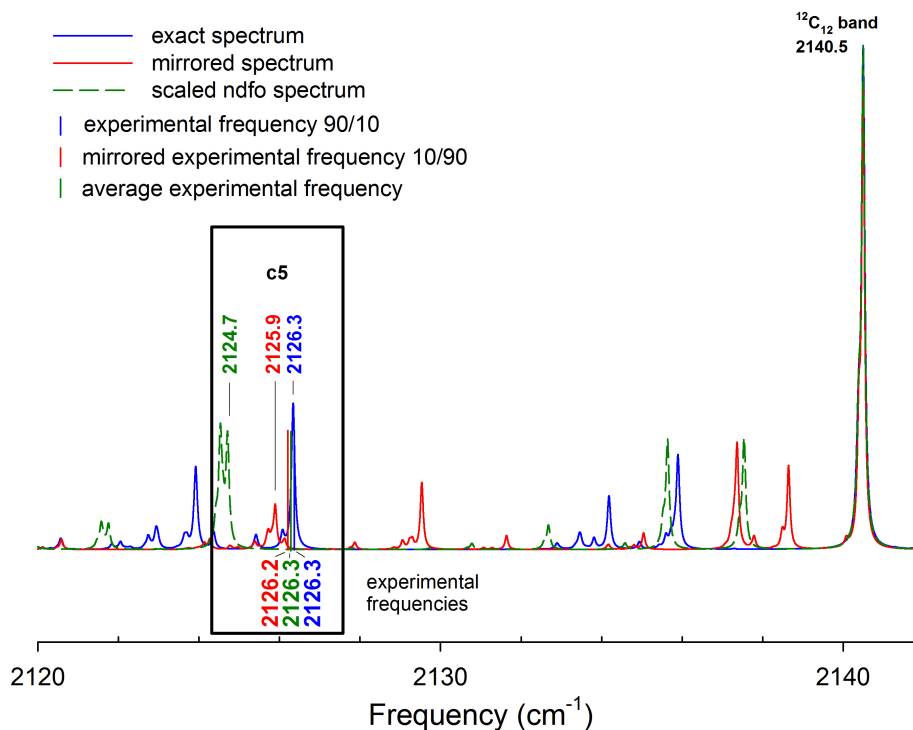


Figure 5. Application of the isotopic deperturbation method to the isotopic spectra of the $\nu_7(\sigma_u)$ mode of linear C_{12} : Isotopic shifts due to substitution on the fifth (c5) molecular site

Finally, Figure 6 shows an example where the isotopic deperturbation method works rather well. The calculated SNDFO isotopic shift for the c6 substitution (green dashed) is approximately equal to the average frequency between the simulated ^{13}C and mirrored- ^{12}C isotopic shifts. This would suggest that the third and higher order terms are not significant in the isotopic shift calculation for the c6 substitution (according to the Eqs. (3.9) and (3.12)). Thus, the coupling effects exhibited by the isotopic shifts of the c6 substitution are mainly produced by the second order contributions.

As defined by the isotopic deperturbation method, the comparison between the SNDFO isotopic shift (green dashed) and the average frequency between the *experimental* ^{13}C and mirrored- ^{12}C isotopic shifts (green bar) does not involve coupling effects from the

second order contributions. Therefore, the discrepancies that appear in the comparison between theoretical and experimental coupling effects do not appear in the comparison between the SNDFO isotopic shift and the average experimental frequency. Actually, a very good agreement between theory and experiment is evident in the later case.

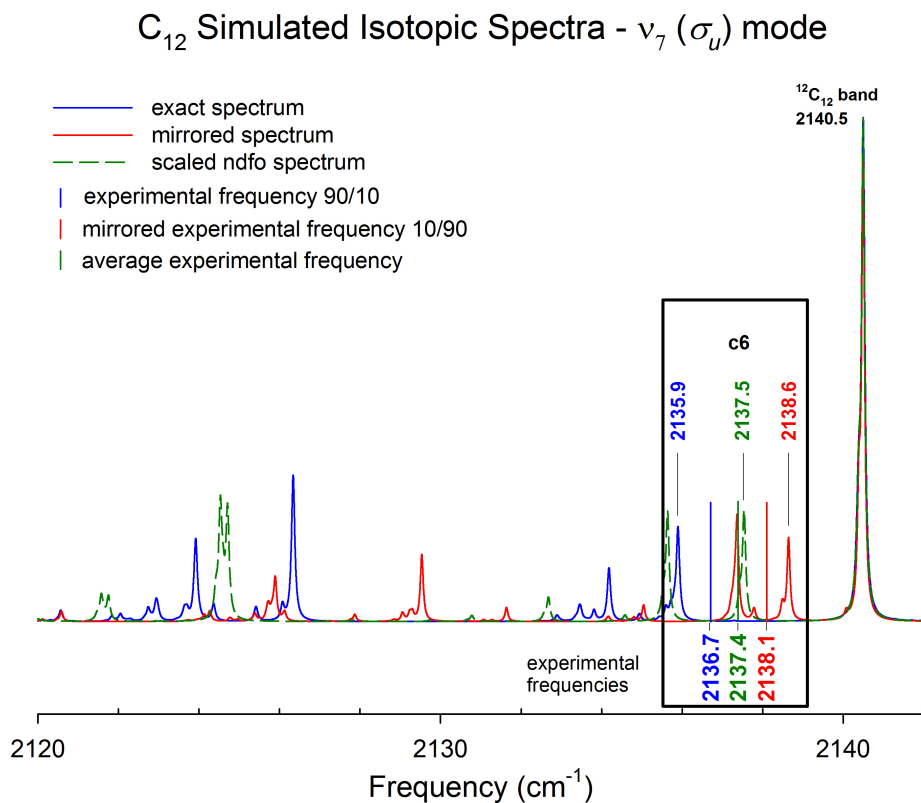


Figure 6. Application of the isotopic deperturbation method to the isotopic spectra of the $\nu_7(\sigma_u)$ mode of linear C_{12} : Isotopic shifts due to substitution on the sixth (c6) molecular site

3.3.3. Linear C_n ($n = 15, 18$)

The applicability of the isotopic deperturbation method has been challenged by the isotopic spectra of these molecules.

Figure 7 and Figure 8* show the isotopic spectra of the $\nu_{10}(\sigma_u)$ mode of linear C_{15} and the $\nu_{12}(\sigma_u)$ mode of linear C_{18} , for different ^{12}C : ^{13}C ratios. The Figures also show the overlapping isotopic spectra of other carbon chains in this frequency range.

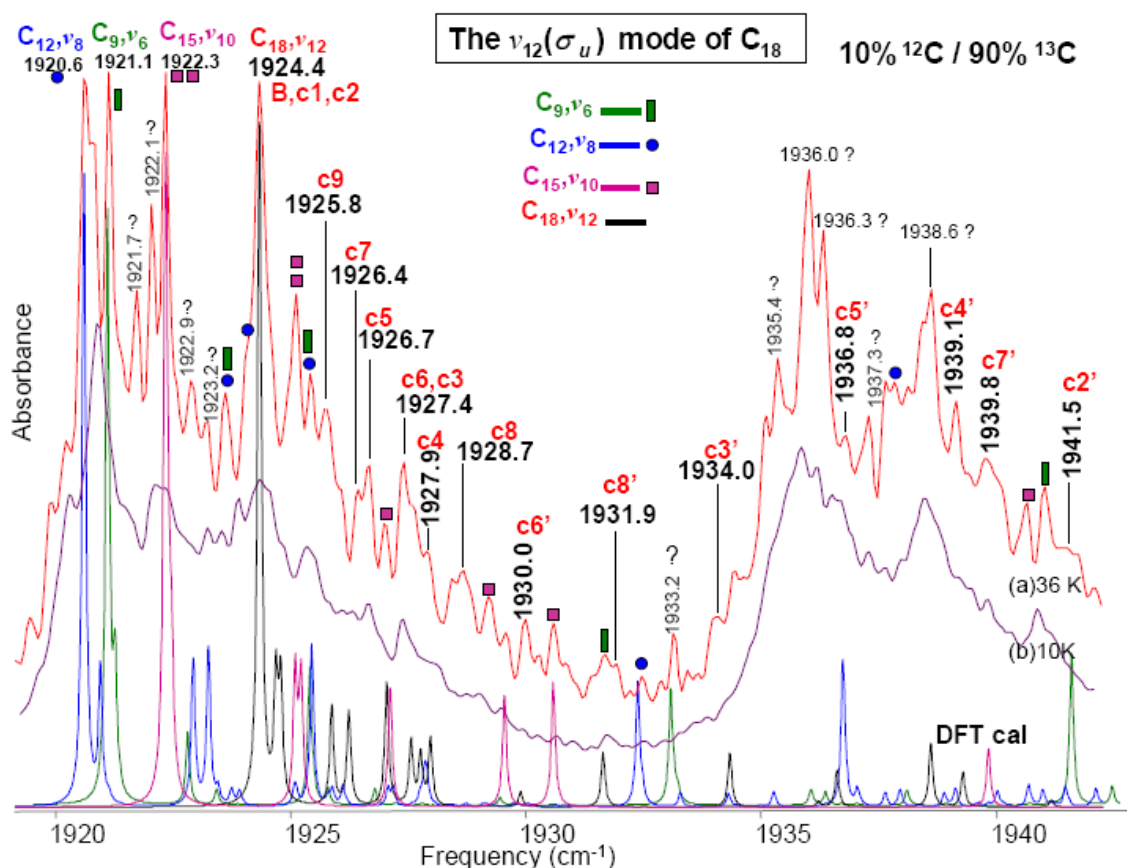


Figure 7. Comparison between the experimental and simulated isotopic spectra of the $\nu_{10}(\sigma_u)$ mode of linear C_{15} and the $\nu_{12}(\sigma_u)$ mode of linear C_{18} . Carbon ratio: 10% ^{12}C / 90% ^{13}C .

* These Figures are courtesy of R. Cárdenas – TCU Molecular Physics Laboratory.

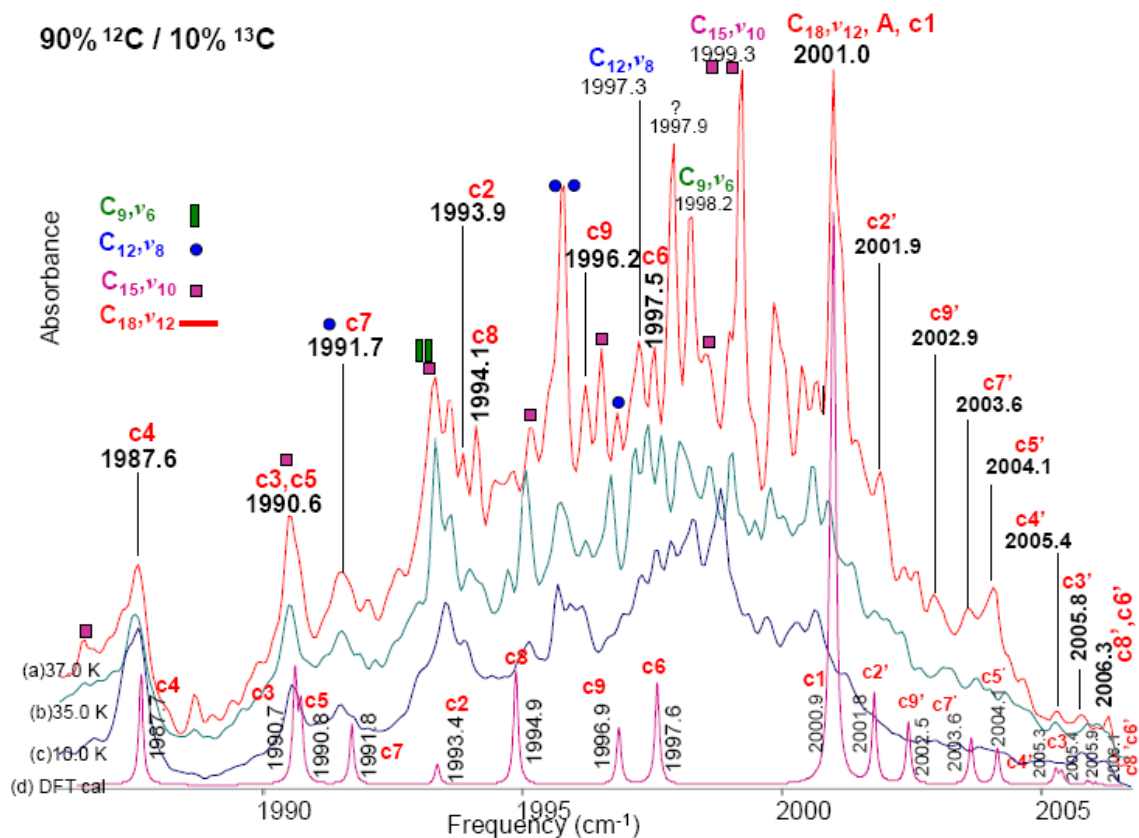


Figure 8. Comparison between the experimental and simulated isotopic spectra of the $\nu_{12}(\sigma_u)$ mode of linear C_{18} . Carbon ratio: 90% ^{12}C / 10% ^{13}C .

The complexity of this case lies in the fact that the experimental isotopic spectra exhibit a large number of absorptions in a short frequency range that correspond to different molecular sources. There are absorptions in the experimental spectra that in some cases can be found within 1 cm^{-1} , which is approximately equal to the uncertainty of the predicted isotopic shifts. This scenario decreases the reliability of the isotopic shift assignment and, as consequence, only tentative assignments of isotopic shifts can be proposed.

The isotopic deperturbation method was applied to the tentative assignments of isotopic shifts proposed by Cárdenas.* In this process, a good agreement was found between the coupling effects exhibited by the experimental and simulated isotopic shifts. Still, this result by itself does not provide enough arguments to consider the proposed assignment as definitive.

3.4. Conclusions

First of all, the application of the isotopic deperturbation method to the infrared isotopic spectra of linear C_n ($n = 3 - 12, 15, 18$) allowed us to confirm that the experimental measurements of isotopic shifts exhibit evidence of coupling effects.

Our initial hypothesis stated that, for molecules with near-lying vibrational fundamentals, the calculation of isotopic shifts to second order in perturbation theory is highly sensitive. The second order contributions for these molecules are more significant, and the uncertainties of the calculated harmonic frequencies and normal mode displacements, which are involved in the second order calculations, also become more significant.

Our results obtained with the application of the isotopic deperturbation method seem to support our hypothesis. On the one hand, the results obtained for the first group of linear molecules (C_n , $n = 3 - 6$) showed that these molecules, having “well separated” vibrational fundamentals, do not exhibit significant discrepancies between the experimental and predicted coupling effects. On the other hand, the application of the method to the second group of carbon chains C_n ($n = 7 - 12$) allowed us to observe the high sensitivity in the prediction of coupling effects, when vibrational fundamentals are close in frequency.

* Experimental justification of the selection of isotopic shifts can be found in Ref. 40.

The $\nu_7(\sigma_u)$ mode of linear C_{12} was a clear example of this situation, in which the predicted and experimental coupling effects were not always in good agreement.

Still, comparing theory and experiment in terms of coupling effects was more effective than the “traditional” frequency comparison of vibrational fundamentals and isotopic shifts. The significance of comparing experimental and theoretical isotopic spectra in terms of the coupling effects is the following: In the process of comparing simultaneously the experimental and theoretical isotopic shifts of two analogous vibrational systems, all $^{12}C_n$ and all $^{13}C_n$ species, we are actually verifying that the discrepancies between theory and experiment are similar for both systems. The consistency of these discrepancies is expected since the same approximations are taken into account for the isotopic shift calculation of both systems.

Finally, the applicability of the isotopic deperturbation method was challenged by the isotopic spectra of linear C_n ($n = 15, 18$). The large number of absorptions in the experimental isotopic spectra of these molecules, representing potential candidates of isotopic shifts, exceeded the current accuracy of the predicted isotopic shifts to determine the assignment. Still, the interpretation of the isotopic spectra from an experimental perspective, in combination with the application of the isotopic deperturbation method, provided elements to determine the assignment of the isotopic spectra of these long chains, C_{15} and C_{18} .

The clear evidence of anharmonic effects that was found in the isotopic spectra of linear C_3 , after the application of the isotopic deperturbation method, initiated our interest in studying the effects of anharmonicity on the calculation of isotopic shifts.

CHAPTER IV. ANHARMONICITY

4.1. Introduction

Little is known about the anharmonic effects in the vibrational spectra of carbon clusters. Vala and coworkers^{46,47} have deduced anharmonic spectroscopic constants from the observation of overtones and combination bands of shorter linear carbon clusters. But these studies do not provide direct information about the unperturbed harmonic and the perturbed experimentally observed frequency.

A few theoretical studies have been presented where anharmonic corrections are calculated, typically by including corrections due to the cubic and quartic force fields. Martin and Taylor *et al.* have presented coupled cluster calculations for linear C_3 ⁴⁸ and cyclic C_4 ⁴⁹ and more recently Massó *et al.*⁵⁰ presented a study of linear C_5 including evaluation of the anharmonicity using multiconfigurational second order perturbation theory.

Botschwina and coworkers have presented anharmonic frequencies for C_3 ⁵¹ and C_5 ⁵² and have more recently (see ref. 53 and references therein) performed a systematic study using the coupled cluster method and large basis sets of the structure and vibrational spectra of the carbon chains C_{2n+1} . Together with known experimental frequencies, Botschwina's studies provide the first evidence of the actual magnitude of anharmonic corrections to vibrational fundamentals of such clusters in a systematic way.

To obtain estimates of the anharmonicity directly from the observed spectra and without data from theoretical calculations we here propose a method based on the isotopic effect. Results based on existing isotopic data for carbon clusters along with comparisons

with theoretical calculations of the anharmonicity show the viability of the method. To the author's knowledge the results presented here represent the first experimentally derived estimates of the anharmonicity of carbon clusters.

4.2. Theory

The theoretical background introduced in Chapter II will be employed in order to develop the method introduced here. In this section we will first find how the perturbative anharmonic corrections for homonuclear systems scale with a uniform change in nuclear mass. Subsequently, an expression independent of any calculation of a harmonic force constant matrix, with which we can estimate the anharmonic correction of vibrational fundamentals from isotopic spectra, is derived.

4.2.1. Derivation of Mass-Reduced Perturbation Expressions

In order to proceed we need to find out how the anharmonic contributions to the frequency shift scale as a function of a uniform change of the mass of a homonuclear system. To do so we first derive mass-reduced expressions for the perturbation due to the various terms of the Taylor expansion of the perturbing potential.

We will here assume that we are studying a homonuclear system undergoing a uniform isotopic mass substitution. In this case, the expression (2.5) for calculating harmonic fundamental frequencies can be written as

$$\boldsymbol{\omega}^2 = m^{-1} \mathbf{U} \mathbf{F}_x \mathbf{U}^\dagger \equiv m^{-1} \tilde{\boldsymbol{\omega}}^2 \quad (4.1)$$

where we for future use have defined the “mass-reduced” frequency, $\tilde{\omega}$. In what follows we will denote other quantities for homonuclear systems by a tilde superscript when the mass-dependency has been extracted. The simple relation between the two frequencies in

Eq. (4.1) is the key to deduce information about the anharmonicity from experiment without any prior knowledge of the *harmonic* frequency.

The anharmonic terms of the Taylor expansion of the potential can be expressed in normal mode coordinates

$$W_{anh}(Q_1, Q_2, \dots) = \sum_{p=3}^{\infty} W_{anh}^{[p]} \quad (4.2)$$

$$W_{anh}^{[p]} = \frac{1}{p!} \sum_{ijk\dots} f_{ijk\dots}^{(p)} Q_i Q_j Q_k \dots \quad ; \quad f_{ijk\dots}^{(p)} = \left. \frac{\partial^p V}{\partial Q_i \partial Q_j \partial Q_k \dots} \right|_{equilibrium}$$

In order to conveniently calculate the mass scaling of the perturbative corrections we rewrite the perturbation using what we know about the mass scaling property of the harmonic frequency

$$Q_i = \sqrt{\frac{1}{2\omega_i}} (a_i^\dagger + a_i) = m^{1/4} \sqrt{\frac{1}{2\tilde{\omega}_i}} (a_i^\dagger + a_i) \equiv m^{1/4} \tilde{Q}_i \quad (4.3)$$

Hence

$$W_{anh}^{[p]} = \frac{m^{p/4}}{p!} \sum_{ijk\dots} f_{ijk\dots}^{(p)} \tilde{Q}_i \tilde{Q}_j \tilde{Q}_k \dots \quad (4.4)$$

To find the mass-dependence of the coefficients $f_{ijk\dots}^{(p)}$ we first note that the normal mode matrix \mathbf{U} in Eq. (2.5) is unitary and real. For a homonuclear system it is furthermore independent of a uniform change of mass [see Eq. (4.1)]. We can therefore invert the expression that defines the normal mode coordinates Q_i , which are linear combinations of the Cartesian coordinates x_j , mass-weighted by the nuclear masses m_j

$$Q_i = \sum_j u_{ij} q_j = \sum_j u_{ij} m_j^{1/2} x_j \quad (4.5)$$

Thus

$$x_j = m^{-1/2} \sum Q_k u_{kj} \quad (4.6)$$

so that

$$\frac{\partial}{\partial Q_i} = \sum_j \frac{\partial}{\partial x_j} \frac{\partial x_j}{\partial Q_i} = m^{-1/2} \sum_j \frac{\partial}{\partial x_j} u_{ij} \quad (4.7)$$

and

$$f_{ijk\dots}^{(p)} = m^{-p/2} \left(\sum_{rst\dots} \frac{\partial^p V}{\partial x_r \partial x_s \partial x_t \dots} u_{ir} u_{js} u_{kt} \dots \right) \Big|_{\text{equilibrium}} \equiv m^{-p/2} \tilde{f}_{ijk\dots}^{(p)} \quad (4.8)$$

Using Eqs. (4.2), (4.4), and (4.8) we now find that the p 'th term of the Taylor expansion scales as

$$m^{p/4} m^{-p/2} = m^{-p/4} \quad (4.9)$$

and we can rewrite the anharmonic terms of the Taylor expansion of the potential (4.2) in terms of contributions, $\tilde{W}_{anh}^{[p]}$, which are independent of the mass parameter m

$$W_{anh}(Q_1, Q_2, \dots) = m^{-3/4} \tilde{W}_{anh}^{[3]} + m^{-1} \tilde{W}_{anh}^{[4]} + \dots = \sum_{p=3}^{\infty} m^{-p/4} \tilde{W}_{anh}^{[p]} \quad (4.10)$$

$$\tilde{W}_{anh}^{[p]} = \frac{1}{p!} \sum_{ijk\dots n} \tilde{f}_{ijk\dots}^{(p)} \tilde{Q}_i \tilde{Q}_j \tilde{Q}_k \dots$$

4.2.2. Mass Scaling of RSPT for Harmonic Oscillators

The anharmonic correction to the frequency due to perturbation in Eq. (4.10) can be analyzed by use of Rayleigh-Schrödinger perturbation theory (RSPT). Here we again assume a homonuclear system undergoing a uniform mass perturbation.

The bracketing theorem (see Ref. 62) gives a compact representation of the order-by-order frequency corrections in non-degenerate RSPT to a state $|n\rangle$. Defining

$\langle W \rangle = \langle n | W | n \rangle$ we have that

$$\begin{aligned}
\omega^{(1)} &= \langle W \rangle \\
\omega^{(q)} &= \langle W (RW)^{q-1} \rangle + \mathfrak{R}^{(q)} \\
R &= \sum_{l \neq n} \frac{|l\rangle\langle l|}{E_n - E_l}
\end{aligned} \tag{4.11}$$

where the *renormalization* term, $\mathfrak{R}^{(q)}$, contains the same powers of W and R as does the *principal* term. Since the harmonic energy levels of our system depend linearly on the harmonic frequencies we have that the resolvent for our system scales with mass as

$$R = \sum_{l \neq n} \frac{|l\rangle\langle l|}{E_n - E_l} = m^{1/2} \sum_{l \neq n} \frac{|l\rangle\langle l|}{\tilde{E}_n - \tilde{E}_l} \tag{4.12}$$

Given the scaling properties of the various terms in the anharmonic perturbation given by Eq. (4.10), and the resolvent given in Eq. (4.12), it is straightforward to apply the bracketing theorem to deduce the mass scaling property of the remaining contributions to the anharmonicity.

We will focus here on the cubic and quartic terms in the expansion of the potential and their contributions up to second order as is typical for perturbative treatment of the anharmonicity (see Ref. 41). Using Eqs. (4.10) - (4.12) we can easily find how these corrections scales with the uniform change in mass.

In first order only the quartic term of the potential contributes and we find

$$m^{-1} \langle n | \tilde{W}_{anh}^{[4]} | n \rangle \tag{4.13}$$

In second order we get contributions from both potential terms but since they involve couplings with different excitations we can treat them separately. For the cubic term we find

$$m^{1/2} \sum_{l \neq n} \frac{\langle n | m^{-3/4} \tilde{W}_{anh}^{[3]} | l \rangle \langle l | m^{-3/4} \tilde{W}_{anh}^{[3]} | n \rangle}{\tilde{E}_n - \tilde{E}_l} = m^{-1} \sum_{l \neq n} \frac{\langle n | \tilde{W}_{anh}^{[3]} | l \rangle \langle l | \tilde{W}_{anh}^{[3]} | n \rangle}{\tilde{E}_n - \tilde{E}_l} \tag{4.14}$$

where the mass-dependence in the summation on the right-hand side has been removed.

Similarly we find that the quartic contribution to second order scales as

$$m^{1/2} \sum_{l \neq n} \frac{\langle n | m^{-1} \tilde{W}_{anh}^{[4]} | l \rangle \langle l | m^{-1} \tilde{W}_{anh}^{[4]} | n \rangle}{\tilde{E}_n - \tilde{E}_l} = m^{-3/2} \sum_{l \neq n} \frac{\langle n | \tilde{W}_{anh}^{[4]} | l \rangle \langle l | \tilde{W}_{anh}^{[4]} | n \rangle}{\tilde{E}_n - \tilde{E}_l} \quad (4.15)$$

To second order in perturbation theory the contributions from the cubic and quartic terms for a particular vibrational energy level E_n can now be written as

$$\delta E_n^{(2)}(m) = m^{-1} \left[\langle n | \tilde{W}_{anh}^{[4]} | n \rangle + \sum_{l \neq n} \frac{\langle n | \tilde{W}_{anh}^{[3]} | l \rangle \langle l | \tilde{W}_{anh}^{[3]} | n \rangle}{\tilde{E}_n - \tilde{E}_l} + m^{-1/2} \sum_{l \neq n} \frac{\langle n | \tilde{W}_{anh}^{[4]} | l \rangle \langle l | \tilde{W}_{anh}^{[4]} | n \rangle}{\tilde{E}_n - \tilde{E}_l} \right] \quad (4.16)$$

To proceed we will assume that the quartic contribution to second order is sufficiently small to warrant us to write the *approximate* anharmonic correction to an energy level to second order as

$$\delta E_n^{(2)}(m) \square m^{-1} \left[\langle n | \tilde{W}_{anh}^{[4]} | n \rangle + \sum_{l \neq n} \frac{\langle n | \tilde{W}_{anh}^{[3]} | l \rangle \langle l | \tilde{W}_{anh}^{[3]} | n \rangle}{\tilde{E}_n - \tilde{E}_l} + \sum_{l \neq n} \frac{\langle n | \tilde{W}_{anh}^{[4]} | l \rangle \langle l | \tilde{W}_{anh}^{[4]} | n \rangle}{\tilde{E}_n - \tilde{E}_l} \right] \quad (4.17)$$

We also note that approximate scaling property in Eq. (4.17) also holds in a perturbative treatment of degenerate or near degenerate cases.

In what follows we will only be interested in the ratio of the anharmonic correction given in Eq. (4.16) for two different values of the mass parameter

$$\frac{\delta E_n^{(2)}(m')}{\delta E_n^{(2)}(m)} = \left(\frac{m'}{m} \right)^{-1} \equiv \gamma^2 \quad (4.18)$$

The explicit value of the quantity in parenthesis in the right-hand side of Eq. (4.16) is therefore not of interest here although this is the quantity necessary to be able to *calculate* the perturbative anharmonic correction.

4.2.3. Derivation of Anharmonic Isotopic Shift Expressions

Knowing how the harmonic frequency as well as the anharmonic perturbation contributions scale as a function of a uniform mass change now gives us a way to derive an expression by which we can estimate the anharmonicity from experimental isotopic data. Since a transition frequency depends on the energy difference between two vibrational states and therefore scales the same way as the energy with respect to a uniform change in mass, Eq. (4.18) gives that the anharmonic correction to the frequency for our system fulfills

$$\frac{\delta\omega(m')}{\delta\omega(m)} = \gamma^2 \quad (4.19)$$

Based on our assumption that Eq. (4.17) describes the dominating anharmonic effects we have that the anharmonic frequency for a given mass parameter m is given by

$$\nu(m) = \omega(m) + \delta\omega(m) \quad (4.20)$$

where $\nu(m)$ denotes the anharmonic frequency and $\omega(m)$ the harmonic frequency for a specific mass m . Using Eqs. (4.1) and (4.19) we find that for a different value of the mass parameter

$$\nu(m') = \omega(m') + \delta\omega(m') = \gamma\omega(m) + \gamma^2\delta\omega(m) \quad (4.21)$$

Multiplying Eq. (4.20) by γ and subtracting Eq. (4.21) we find

$$\gamma\nu(m) - \nu(m') = \gamma\delta\omega(m) - \gamma^2\delta\omega(m) \equiv \Delta \quad (4.22)$$

We identify Δ as the difference between the frequency $\gamma\nu(m)$ and the anharmonic isotopic frequency $\nu(m')$, where $\gamma\nu(m)$ represents the isotopic frequency due to the mass change $m \rightarrow m'$ that would result if $\nu(m)$ is assumed to be the harmonic frequency. Solving for the anharmonic shift we find

$$\delta\omega(m) = \frac{\Delta}{\gamma - \gamma^2} \quad (4.23)$$

The quantity Δ can be readily obtained from an isotopic spectrum for a homonuclear system provided frequencies are available for the two masses m and m' . Eq. (4.23) hence provides a way to obtain the anharmonicity of a given vibrational fundamental directly from experimental data without any prior knowledge of the harmonic frequency.

4.3. Application and Discussion

We first present linear C_3 as an example where the analysis of the anharmonic effect just described can be applied. The top part of Figure 9 shows the isotopic spectrum observed for the $\nu_3(\sigma_u)$ fundamental of C_3 using a $^{12}C/^{13}C$ isotopic ratio of approximately 50%/50%. The bottom part of the same figure shows the simulated harmonic spectrum using density functional theory (DFT) with the B3LYP functional and the cc-pVDZ basis set. The calculated spectrum has been scaled so that the main full ^{12}C absorption labeled (12-12-12) coincides with the experimental value.

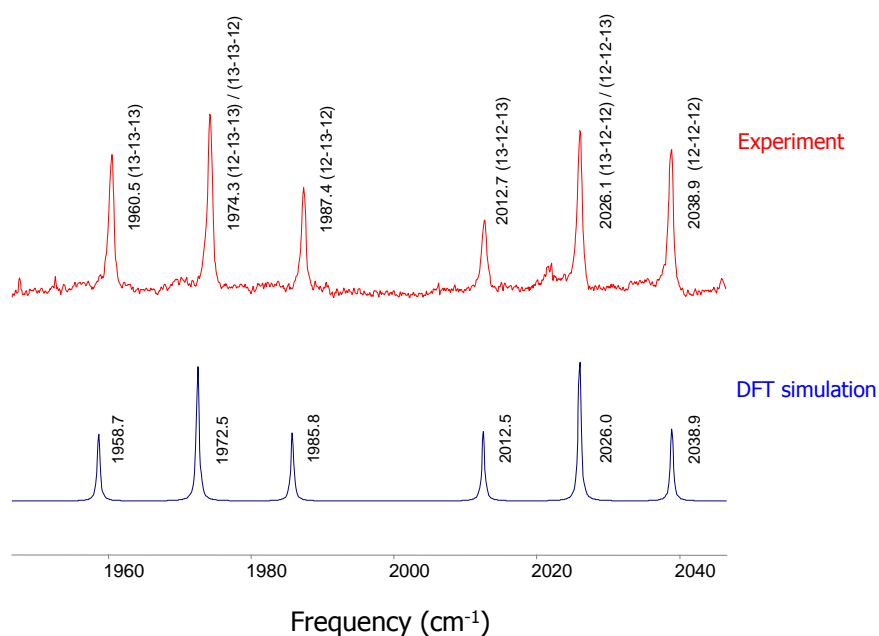


Figure 9. Experimental (top) and DFT simulated (bottom) isotopic spectra for linear C_3 . The isotopic identification for each absorption is given in parenthesis next to the experimental frequency.

In the case of linear C_3 we have the situation that the normal mode coordinates for the $\nu_1(\sigma_g)$ and $\nu_3(\sigma_u)$ modes are completely determined by center of mass and orthonormality constraints. Since the central carbon atom shows no displacement due to symmetry in the σ_g mode we have that $\bar{u}_{central}(\sigma_g) \square \bar{u}_{central}(\sigma_u) = 0$ for this particular isotopic substitution. Furthermore, $\bar{u}_n(\pi) \square \bar{u}_n(\sigma) = 0$ since these normal mode displacements for stretching and bending fundamentals are always orthogonal. The perturbation for the (12-13-12) substitution is therefore completely decoupled from the other vibrational modes, and taking the (12-12-12) absorption to be the *harmonic* frequency, we find that the isotopic perturbation in this case reduces to the following form, which was introduced in Section 2.4.3 by Eq. (2.40)

$$W_{iso}(m \rightarrow m') = \sum_n \lambda(m \rightarrow m') \frac{\omega_t}{4} |\bar{u}_n(t)|^2 (a_t^\dagger - a_t)^2$$

$$+ \sum_{rs \neq t} \sum_n \lambda_n(m \rightarrow m') \frac{\sqrt{\omega_r} \sqrt{\omega_s}}{4} \bar{u}_n(r) \bar{u}_n(s) (a_r^\dagger - a_r)(a_s^\dagger - a_s)$$

If there were no anharmonicity in this vibrational mode we would therefore expect the calculated (12-13-12) isotopic shift to be accurate. The discrepancy seen in Figure 9 between the calculated and experimental value for the (12-13-12) absorption is therefore an illustration of an anharmonic effect. We note that for other single and double ^{13}C substitutions in the (12-12-12) isotopomer the $\nu_3(\sigma_u)$ would couple with the $\nu_1(\sigma_g)$ mode but since the harmonic frequency is not known, the discrepancy between theory and experiment in this case can not immediately be attributed to anharmonicity.

To get an estimate of the anharmonicity of the full ^{12}C isotopomer (12-12-12) we now turn to Eqs. (4.22) and (4.23). In the case of a full ^{13}C substitution all modes are completely decoupled in the harmonic approximation due to the orthonormality of normal modes and we can apply Eq. (2.42), given by

$$\omega'_t = \left(\frac{m'}{m} \right)^{1/2} \omega_t$$

The scaled DFT simulation along with the experimentally observed value for the full ^{13}C (13-13-13) absorption gives us the input necessary to calculate Δ defined in Eq. (4.22), which together with knowledge of the participating nuclear masses subsequently gives us the estimated anharmonicity from Eq. (4.23). Referring to Figure 9 we find explicitly that with the mass ratio $\gamma^2 = 12/13.00335$ we have that $\Delta = 1958.66 - 1960.2 = -1.54 \text{ cm}^{-1}$ resulting in an anharmonicity for the $\nu_3(\sigma_u)$ fundamental transition of linear C_3 of about -49 cm^{-1} .

This approach is applicable to any situation where the full ^{12}C and ^{13}C absorptions for a given carbon cluster are known from experiment. Such data has been accumulated by our group in the course of identifying new vibrational fundamentals of both linear and cyclic carbon clusters in matrix isolation using Fourier transform infrared spectroscopy. The clusters are generated by laser ablation of carbon rods, which are made with specific isotopic ratios in order to create infrared spectra with the isotopic “fingerprints” of a particular cluster.⁴⁰ Here we will focus on our experimental data for linear carbon chains (C_{2n+1} ; $n=1-6$)^{27,29,30,40} and presented here for C_3 . We also include the experimentally derived anharmonicity for the cyclic carbon clusters C_6 ^{32,33} and C_8 .⁵⁴ In order to validate such experimentally derived results we also calculated theoretical estimates of the anharmonicity of the linear stretching modes of carbon chains (C_{2n+1} ; $n=1-6$) using density functional theory (DFT) with the B3LYP^{55,56,57} functionals and cc-pVDZ⁵⁸ basis sets as implemented in the Gaussian 03⁴⁴ program suite. The current Gaussian implementation of the perturbative calculation of anharmonic vibrational properties¹⁸ is however unable to handle anharmonicities involving degenerate point groups. To obtain results for the non-degenerate stretching modes of linear chains we therefore distorted the central atom of each chain about 0.001 Ångström perpendicular to the symmetry axis and the calculation was performed in C_{2v} symmetry. The resulting changes in the calculation of the properties considered here are negligible but serve to “fool” the program into performing the calculation.

Table 2 shows the results for the anharmonicity derived from our experimental data along with B3LYP/cc-pVDZ values (for linear clusters) and theoretical results based on more extensive treatments for C_3 ^{48,51} and C_5 .^{50,52} Given the uncertainties involved in the

calculated anharmonicities as well as the inaccuracy in the frequency measurement, reasonable agreement is obtained between the values derived from the isotopic experimental data and the theoretical predictions. In most cases the B3LYP/cc-pVDZ values are lower than those derived exclusively from experiment using the present technique. In the case of C_3 where the difference between these values is particularly large it is reassuring to see that the theoretical values resulting from more sophisticated calculations agree very well with our experimentally derived result. This serves as a nice benchmark of our approach since the $\nu_3(\sigma_u)$ anharmonic frequency calculated in refs. 48 and 51 is within a few cm^{-1} of the experimental result obtained in the gas phase.

Ideally, the required isotopic data should be obtained in the gas phase since matrix effects would in principle need to be considered. For the fundamentals considered here the (red) shift due to the matrix ranges from a few to about 15 cm^{-1} (for the $\nu_5(\sigma_u)$ mode of C_9). Considering the matrix environment as an *external* perturbation expanded in normal mode coordinates one finds that matrix contributions due to quadratic terms scales as $m^{-1/2}$ and therefore cancel to second order in Eq. (4.22). The matrix contribution due to cubic and quartic terms would have the same scaling properties as the *internal* anharmonicity and would therefore contribute in the calculation of $\delta\omega(m)$ in Eq. (4.23).

Table 2. Comparison of values of the anharmonicity from calculation and experiment. All values are in cm^{-1} .

	B3LYP/cc-pVDZ		Experiment ^c			Ref.
	ω	$\delta\omega$	$\nu(^{12}\text{C})$	$\nu(^{13}\text{C})$	$\delta\omega^{(*)}$	
C_3						
$\nu_3(\sigma_u)$	<u>2157.8</u>	-33	2038.9	1960.2	-49	-51 ^a , -58 ^b
C_5						
$\nu_3(\sigma_u)$	<u>2269.8</u>	-40	2164.3	2080.5	-36	-21 ^c , -29 ^d
$\nu_4(\sigma_u)$	1498.9	-15	1446.6	1390.2	-14	-11 ^c , -16 ^d
C_7						
$\nu_4(\sigma_u)$	<u>2258.1</u>	-34	2127.8	2045.8	-46	
$\nu_5(\sigma_u)$	1988.3	-28	1894.3	1821.0	-36	
C_9						
$\nu_5(\sigma_u)$	2217.6	-32	2078.1	1998.1	-47	
$\nu_6(\sigma_u)$	<u>2132.6</u>	-37	1998.0	1921.1	-46	
$\nu_7(\sigma_u)$	1670.0	-18	1601.0	1538.8	-21	
C_{11}						
$\nu_7(\sigma_u)$	<u>2126.3</u>	-33	1942.6	1868.0	-49	
$\nu_8(\sigma_u)$	1946.9	-30	1854.8	1783.1	-34	
$\nu_9(\sigma_u)$	1404.5	-14	1357.0	1304.1	-13	
C_{13}						
$\nu_9(\sigma_u)$	<u>2039.8</u>	-33	1809.0			
cyc- C_6						
$\nu_4(e')$	<u>1769.6</u>		1694.9	1630.5	-52	
cyc- C_8						
$\nu_{12}(e_u)$	<u>1932.9</u>		1844.2	1774.4	-51	

(*) Anharmonicity calculated using Eq. (4.23). The error due to the inaccuracy of about 0.1 cm^{-1} in the experimental frequency values translates into an inaccuracy of about $\pm 4 \text{ cm}^{-1}$ in these values.

^a Ref. 48 ^b Ref.52 ^c Ref. 50 ^d Ref. 51

^e Experimental data from refs. 27, 29, 30, 32, 33, 40, 54; except for C_{11} (ref. 59), and C_{13} (ref. 60). For each cluster the frequency with the highest infrared intensity is underlined.

Since the anharmonicity is also given by the difference between the true harmonic and the experimental frequencies ($\omega - \nu$) an alternate way of obtaining this value is to seek to calculate the best possible approximation of the true harmonic frequency and compare this with experiment. Recently Botschwina⁵³ presented such a comparison based on high level coupled cluster calculations including triple excitations and up to valence-quadruple-zeta basis sets for harmonic frequencies of linear C_{2n+1} chains. In particular he presented a graph where $(\omega - \nu)$ for the modes of highest infrared intensity was plotted as function of n , for $n=1-9$. The experimental data for $n=1-4$ coincides with the data presented here (see Table 2). In addition, Botschwina included the assignments from nitrogen matrix experiments for linear C_{11} by Lapinski and Vala,⁵⁹ for linear C_{13} obtained in the gas phase by Giesen *et al.*,⁶⁰ as well as some recent assignments for linear C_{15} , C_{17} , and C_{19} by Strelnikov *et al.*⁶¹ from laser-induced oxidation experiments. In Figure 10 we present a similar plot where our estimates of the anharmonicity deduced from experiments are shown for $n=1-5$, as well as our B3LYP/cc-pVDZ data for $n=1-6$, for the most intense vibrational fundamentals of C_{2n+1} . Our results in Table 2 and Figure 10 compare very well with those of Botschwina for $n=1-4$. However, our calculated anharmonicities using B3LYP/cc-pVDZ remain nearly constant also for linear C_{11} and C_{13} (see Figure 10), whereas Botschwina found an onset of a rather dramatic increase in his values for $(\omega - \nu)$ for these and longer chains going from around 50 - 70 cm^{-1} for $C_3 - C_9$, to 300 cm^{-1} for C_{19} .

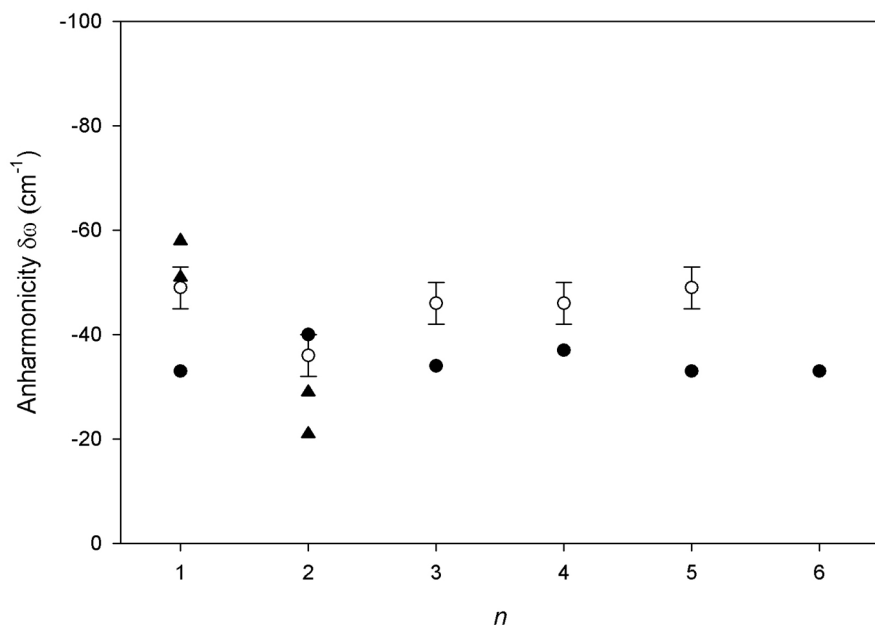


Figure 10. Experimentally derived (open circles) estimates of the anharmonicity for the most intense fundamentals of linear carbon chains C_{2n+1} . Filled circles correspond to the B3LYP/cc-pVDZ results in this work. Triangles refer to existing theoretical predictions in the literature (see Table 2 for details).

An additional illustration of the need of further investigations to resolve these issues is illustrated in Figure 11. Here we have plotted the experimental frequencies for C_{2n+1} ($n=1-4$) carbon chains from our work against the B3LYP/cc-pVDZ anharmonic results presented in Table 2. We have also included our DFT based data with the experimental assignments by other investigators for linear C_{11} and C_{13} . The data for $n=1-4$ is well represented by the linear fit:

$$\nu(\text{observed}) \approx 0.92673\nu(\text{anharmonic-B3LYP/cc-pVDZ}) + 70.3 \text{ cm}^{-1}$$

Also, the data for the $\nu_8(\sigma_u)$ and $\nu_9(\sigma_u)$ modes of C_{11} fall along the same fit whereas the most intense bands for C_{11} , ($\nu_7(\sigma_u)$), and C_{13} , ($\nu_9(\sigma_u)$), do not. This mirrors Botschwina's

observation of a dramatic increase in $(\omega - \nu)$ beginning for the bands identified with the most intense fundamentals of these clusters.

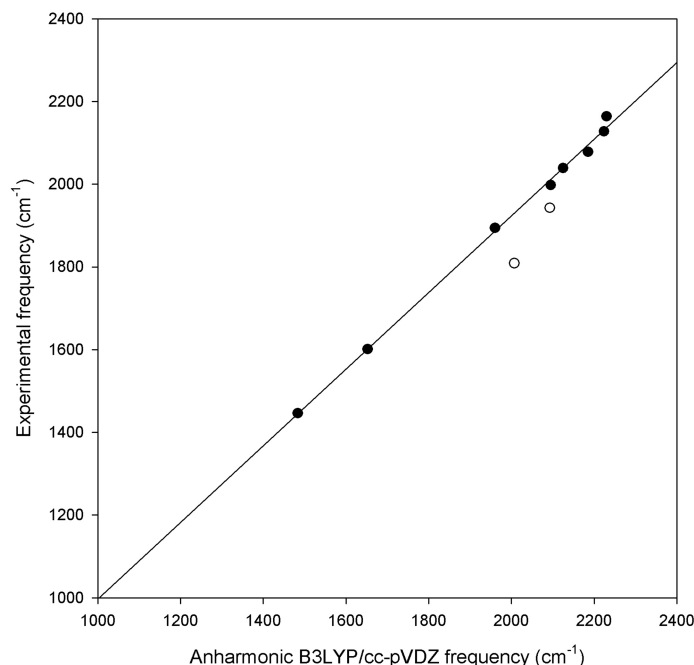


Figure 11. Experimentally observed stretching fundamental frequencies for linear carbon chains C_{2n+1} ($n=1-4$) vs. the calculated anharmonic B3LYP/cc-pVDZ frequency using the data in Table 2 (filled circles). The open circles represent the same data for the observed fundamentals of linear C_{11} and C_{13} (see text for discussion).

We also note that Strelnikov *et al.* associates an absorption at 1695 cm^{-1} with the most intense fundamental of linear C_{15} . This would be a reassignment of the absorption that we previously assigned to cyclic C_6 . Botschwina's CCSD(T) results show a difference $(\omega - \nu)$ of 166 cm^{-1} for the assignment of this absorption to linear C_{15} . From the experimental data presented here (see Table 2) we find the anharmonicity of this mode to be -52 cm^{-1} . Since the way the value of the anharmonicity derived here is independent of the identity of the particular cluster, the difference between these numbers, along with the

isotopic data for single isotopic shifts presented in our original identification,³² lends support to our assignment of cyclic C₆ to the 1695 cm⁻¹ absorption.

4.4. Conclusions

A new method by which to obtain estimates of the anharmonicity of homonuclear molecules has been presented. The method is based entirely on the observation of the isotopic shift resulting from a uniform change of all atomic masses. In particular, anharmonicities for carbon clusters can be obtained by observing the isotopic shift upon full ¹³C substitution. Existing isotopic data for linear carbon chains C_{2n+1}, n=1-5 was used to illustrate the applicability of the approach. Good agreement was found between the results obtained by the new method and published as well as new DFT calculations. The results further illustrate the existing discrepancy between theoretical predictions of vibrational fundamentals of longer carbon chains and experimental assignments and therefore reiterate the call for further studies for their resolution.

CHAPTER V. CONCLUSIONS AND FUTURE WORK

5.1. Conclusions

The present work investigated two theoretical issues related to the calculation of isotopic shifts: *i*) the sensitivity of simulated isotopic spectra due to the interaction of vibrational fundamentals and *ii*) the sensitivity of simulated isotopic spectra due to the anharmonicity of the interaction potential. These issues affect more the calculations of molecules with near-lying vibrational fundamentals and represent the cause of the observed disagreement in the comparison between isotopic shift calculations and experimental measurements.

Two theoretical approaches, developed in the framework of perturbation theory, were introduced in the present work as a consequence of investigating the issues aforementioned. Both approaches, applicable to isotopic spectra of homonuclear molecules, were applied to measurements of vibrational fundamentals and isotopic shifts of carbon clusters since some of these molecules ($n \geq 7$) have close-lying vibrational fundamentals; isotopic spectra of long carbon chains exhibit the problems that arise as a consequence of the issues investigated in the present work.

Overall, both theoretical approaches presented here yielded satisfactory results. The isotopic deperturbation method (Chapter III) led to substantial progress in terms of having a deeper understanding of the effects produced by the interactions of vibrational fundamentals, and most importantly, this technique assisted in the interpretation of experimental isotopic spectra despite the sensitivity of the corresponding simulations. Also, the results obtained with the method to estimate anharmonicity of vibrational fundamentals

(Chapter IV) were in good agreement with the existing predictions, as well as with our recent DFT calculations. Indeed, the results obtained with this method provided evidence to question previous assignments of vibrational fundamentals of longer carbon chains.

Finally, it is worth noting the positive repercussion of acquiring isotopic shift measurements of two analogous vibrational systems (like the case of $^{12}\text{C}_n$ and $^{13}\text{C}_n$ chains) since the availability of these complementary sets of measurements contribute to the development of new theoretical methods.

5.2. Future Work

A method to estimate the anharmonicity of vibrational fundamentals from isotopic shift measurements was introduced in the present work. However, it still is necessary to further investigate the quantitative effects of anharmonicity on isotopic shift calculations. Therefore, a key step for this study will be to write a code that allows us to perform numerical calculations of the anharmonicity of isotopic shifts and vibrational fundamentals, by calculating the second order correction in perturbation theory due to the cubic term of the Taylor's series expansion of the potential, as well as the first- and second-order contributions due to the quartic term of this expansion, which is typical for a perturbative treatment of anharmonicity. Thus, more accurate simulations of isotopic spectra can be produced by taking into account anharmonic effects in the calculation of isotopic shifts. This may allow us to achieve a better interpretation of experimental isotopic spectra that is highly "congested" and, specifically, this may also allow us to accomplish the definitive assignment of isotopic shifts in the isotopic spectra presented in Figure 7 and Figure 8.

APPENDICES

A. The Canonical Transformation of the Vibrational Hamiltonian

The nuclear Hamiltonian in the harmonic approximation is given by:

$$H_0 = -\sum_{i=1}^N \frac{1}{2m_i} \nabla_i^2 + \frac{1}{2} \sum_{i=1}^N \sum_{r=1}^3 \sum_{j=1}^N \sum_{s=1}^3 f_{irjs} x_{ir} x_{js} \quad (\text{A.1})$$

Introducing for convenience the mass-weighted coordinates:

$$q_{ir} = \sqrt{m_i} x_{ir} \quad (\text{A.2})$$

Writing the expression (A.2) in matrix form:

$$\mathbf{q} = \mathbf{M}^{1/2} \mathbf{x}. \quad (\text{A.3})$$

Considering that

$$\frac{\partial}{\partial x_{ir}} = \frac{\partial}{\partial q_{ir}} \frac{\partial q_{ir}}{\partial x_{ir}} = \sqrt{m_i} \frac{\partial}{\partial q_{ir}} \quad (\text{A.4})$$

the Laplacian can be written as:

$$\nabla_i^2 = \sum_{r=1}^3 \frac{\partial^2}{\partial x_{ir}^2} = \sqrt{m_i} \sum_{r=1}^3 \frac{\partial^2}{\partial q_{ir}^2} \quad (\text{A.5})$$

Making use of the definition (A.2) and substituting the expression (A.5) in the Hamiltonian

(A.1), we have:

$$H_0 = -\frac{1}{2} \sum_{i=1}^N \sum_{r=1}^3 \frac{\partial^2}{\partial q_{ir}^2} + \frac{1}{2} \sum_{i=1}^N \sum_{r=1}^3 \sum_{j=1}^N \sum_{s=1}^3 \frac{1}{\sqrt{m_i}} \frac{1}{\sqrt{m_j}} f_{irjs} q_{ir} q_{js} \quad (\text{A.6})$$

The Hamiltonian is now expressed in terms of the mass-weighted coordinates.

Introducing the normal mode coordinates, formed by $3N$ linear combinations of the mass-weighted coordinates, we have:

$$\begin{aligned}
Q_{ir} &= \sum_{j=1}^N \sum_{s=1}^3 u(ir)_{js} q_{js} = \sum_{j=1}^N \sum_{s=1}^3 u(ir)_{js} \sqrt{m_j} x_{js} \\
\mathbf{Q} &= \mathbf{U}\mathbf{q} = \mathbf{U}\mathbf{M}^{1/2}\mathbf{x} \\
\mathbf{q} &= \mathbf{U}^\dagger \mathbf{Q} \\
\mathbf{x} &= \mathbf{M}^{-1/2} \mathbf{U}^\dagger \mathbf{Q}
\end{aligned} \tag{A.7}$$

The matrix \mathbf{U} with elements:

$$u(ir)_{js} \tag{A.8}$$

(where the index ir denotes the row and js the column) is chosen to diagonalize the mass-weighted Cartesian Hessian matrix $\mathbf{M}^{-1/2} \mathbf{F}_x \mathbf{M}^{-1/2}$ so that

$$\boldsymbol{\omega}^2 = \mathbf{U}\mathbf{M}^{-1/2} \mathbf{F}_x \mathbf{M}^{-1/2} \mathbf{U}^\dagger \tag{A.9}$$

Besides,

$$\begin{aligned}
\mathbf{U}^\dagger &= \tilde{\mathbf{U}} \\
\mathbf{U}\tilde{\mathbf{U}} &= \mathbf{1}
\end{aligned} \tag{A.10}$$

since the Hessian matrix is real and symmetric.

The kinetic energy operator can be expressed in normal mode coordinates:

$$\begin{aligned}
\frac{\partial}{\partial q_{ir}} &= \sum_j^N \sum_s^3 \frac{\partial}{\partial Q_{js}} \frac{\partial Q_{js}}{\partial q_{ir}} = \sum_{j=1}^N \sum_{s=1}^3 u(js)_{ir} \frac{\partial}{\partial Q_{js}} \\
\frac{\partial^2}{\partial q_{ir}^2} &= \sum_j^N \sum_s^3 \frac{\partial}{\partial Q_{js}} \frac{\partial Q_{js}}{\partial q_{ir}} = \sum_{j=1}^N \sum_{s=1}^3 \sum_{k=1}^N \sum_{t=1}^3 u(js)_{ir} u(kt)_{ir} \frac{\partial}{\partial Q_{js}} \frac{\partial}{\partial Q_{kt}}
\end{aligned} \tag{A.11}$$

From the orthonormality of the vectors u , the kinetic energy operator can be written as:

$$\begin{aligned}
T_0 &= -\frac{1}{2} \sum_{i=1}^N \sum_{r=1}^3 \frac{\partial^2}{\partial q_{ir}^2} = -\frac{1}{2} \sum_{i=1}^N \sum_{r=1}^3 \sum_{j=1}^N \sum_{s=1}^3 \sum_{k=1}^N \sum_{t=1}^3 u(js)_{ir} u(kt)_{ir} \frac{\partial}{\partial Q_{js}} \frac{\partial}{\partial Q_{kt}} \\
&= -\frac{1}{2} \sum_{j=1}^N \sum_{s=1}^3 \frac{\partial^2}{\partial Q_{js}^2}
\end{aligned} \tag{A.12}$$

Additionally, the potential energy given by:

$$V_0 = \frac{1}{2} \sum_{i=1}^N \sum_{r=1}^3 \sum_{j=1}^N \sum_{s=1}^3 \frac{1}{\sqrt{m_i}} \frac{1}{\sqrt{m_j}} f_{irjs} q_{ir} q_{js} \quad (\text{A.13})$$

can also be expressed in normal mode coordinates. Writing the potential energy (A.13) in matrix form:

$$V_0 = \frac{1}{2} \mathbf{q}^\dagger \mathbf{M}^{-1/2} \mathbf{F}_x \mathbf{M}^{-1/2} \mathbf{q} = \frac{1}{2} \mathbf{Q}^\dagger \mathbf{U} \mathbf{M}^{-1/2} \mathbf{F}_x \mathbf{M}^{-1/2} \mathbf{U}^\dagger \mathbf{Q} \quad (\text{A.14})$$

Recalling expression (A.10), this simplifies to:

$$V_0 = \frac{1}{2} \mathbf{Q}^\dagger \mathbf{U} \mathbf{M}^{-1/2} \mathbf{F}_x \mathbf{M}^{-1/2} \mathbf{U}^\dagger \mathbf{Q} = \frac{1}{2} \mathbf{Q}^\dagger \boldsymbol{\omega}^2 \mathbf{Q} = \frac{1}{2} \sum_{j=1}^N \sum_{s=1}^3 k_{js} Q_{js}^2 \quad (\text{A.15})$$

$$k_{js} = \omega_{js}^2$$

Thus, the original Hamiltonian simplifies to a sum of $3N$ harmonic oscillator Hamiltonians:

$$H_0 = -\frac{1}{2} \sum_{j=1}^N \sum_{s=1}^3 \frac{\partial^2}{\partial Q_{js}^2} + \frac{1}{2} \sum_{j=1}^N \sum_{s=1}^3 k_{js} Q_{js}^2 = \sum_{j=1}^N \sum_{s=1}^3 H_{js} \quad (\text{A.16})$$

This is the canonical representation of the nuclear motion in terms of a set of harmonic oscillators. It is important to note that the rotational and translational degrees of freedom are also embedded in the $3N$ harmonic oscillators. Therefore, linear molecules have $3N-5$ vibrational degrees of freedom (vibrational modes), while non-linear molecules have $3N-6$ vibrational degrees of freedom.

B. Perturbation in the Number Representation and Normal Ordered Operators³⁹

As mentioned on the *isotopic mass perturbation* section, the energy correction caused by this perturbation can be conveniently calculated when the perturbation is written in terms of the ladder operators. The ladder operators for each harmonic oscillator in the Hamiltonian (A.16) are defined as (with the mass $m = 1$):

$$\begin{aligned} a_r^\dagger &= \sqrt{\frac{\omega_r}{2}} \left(\hat{Q}_r - \frac{i}{\omega_r} \hat{P}_r \right) \\ a_r &= \sqrt{\frac{\omega_r}{2}} \left(\hat{Q}_r + \frac{i}{\omega_r} \hat{P}_r \right) \end{aligned} \quad (\text{B.1})$$

The position and momentum operators in terms of the ladder operators are:

$$\begin{aligned} \hat{Q}_r &= \sqrt{\frac{1}{2\omega_r}} (a_r^\dagger + a_r) \\ \hat{P}_r &= i\sqrt{\frac{\omega_r}{2}} (a_r^\dagger - a_r) \end{aligned} \quad (\text{B.2})$$

The ladder operators have the following properties:

$$\begin{aligned} [a_r, a_s^\dagger] &= \delta_{rs} \\ [a_r, a_s] &= [a_r^\dagger, a_s^\dagger] = 0 \\ a_r^\dagger |n_r\rangle &= \sqrt{n_r + 1} |n_r + 1\rangle \\ a_r |n_r\rangle &= \sqrt{n_r} |n_r - 1\rangle \\ a_r |0\rangle &= 0 \end{aligned} \quad (\text{B.3})$$

and the (unperturbed) Hamiltonian for a set of harmonic oscillators can be written as:

$$H_0 = \sum_{r=1}^M \omega_r \left(a_r^\dagger a_r + \frac{1}{2} \right). \quad (\text{B.4})$$

On the other hand, recalling from the *isotopic mass perturbation* section the isotopic perturbation is given by:

$$\begin{aligned}
W(i \rightarrow f) &= \sum_{n=1}^K W_n(i \rightarrow f) = \sum_{n=1}^K \left(\frac{1}{2m_n(i)} \nabla_n^2 - \frac{1}{2m_n(f)} \nabla_n^2 \right) = \\
&\frac{1}{2} \sum_{n=1}^K \left(\frac{1}{m_n(i)} - \frac{1}{m_n(f)} \right) \sum_{u=1}^3 \frac{\partial^2}{\partial x_{nu}^2}
\end{aligned} \tag{B.5}$$

and the $3N$ normal coordinates (A.7) were defined in appendix A as:

$$\begin{aligned}
Q_{jr} &= \sum_{k=1}^N \sum_{s=1}^3 u_{ks}(jr) q_{ks} = \sum_{k=1}^N \sum_{s=1}^3 u_{ks}(jr) \sqrt{m_k} x_{ks} \\
\mathbf{Q} &= \mathbf{U}\mathbf{q} = \mathbf{U}\mathbf{M}^{1/2}\mathbf{x} \\
\mathbf{q} &= \mathbf{U}^\dagger \mathbf{Q} = \tilde{\mathbf{U}}\mathbf{Q}
\end{aligned}$$

Here, the indices j, k, l, \dots stand for the atoms of the system, running from 1 to N . The indices r, s, t, \dots are used to represent the three spatial dimensions, running from 1 to 3. Therefore, the combined indices like ir, js run from 1 to $3N$.

Taking this into account, the first and second derivatives with respect to Cartesian coordinates can be written in terms of the normal coordinates:

$$\begin{aligned}
\frac{\partial}{\partial x_{jr}} &= \sum_{k=1}^N \sum_{s=1}^3 \frac{\partial}{\partial Q_{ks}} \frac{\partial Q_{ks}}{\partial x_{jr}} = \sum_{k=1}^N \sum_{s=1}^3 \frac{\partial}{\partial Q_{ks}} u_{jr}(ks) \sqrt{m_j} \\
\frac{\partial^2}{\partial x_{jr}^2} &= \sum_{k=1}^N \sum_{s=1}^3 \frac{\partial}{\partial Q_{ks}} u_{jr}(ks) \sqrt{m_j} \sum_{l=1}^N \sum_{t=1}^3 \frac{\partial}{\partial Q_{lt}} u_{jr}(lt) \sqrt{m_j} = \\
&\sum_{k=1}^N \sum_{s=1}^3 \sum_{l=1}^N \sum_{t=1}^3 m_j u_{jr}(ks) u_{jr}(lt) \frac{\partial}{\partial Q_{ks}} \frac{\partial}{\partial Q_{lt}}
\end{aligned} \tag{B.6}$$

Substituting the expression for the second derivative with respect to Cartesian coordinates in the expression (B.5), we have:

$$\begin{aligned}
W(i \rightarrow f) &= \sum_{n=1}^K W_n(i \rightarrow f) = \\
&= \frac{1}{2} \sum_{n=1}^K \left(\frac{1}{m_n(i)} - \frac{1}{m_n(f)} \right) \sum_{k=1}^N \sum_{s=1}^3 \sum_{l=1}^N \sum_{t=1}^3 m_n(i) u_{nu}(ks) u_{nu}(lt) \frac{\partial}{\partial Q_{ks}} \frac{\partial}{\partial Q_{lt}} = \\
&= \frac{1}{2} \sum_{n=1}^K \sum_{u=1}^3 \sum_{k=1}^N \sum_{s=1}^3 \sum_{l=1}^N \sum_{t=1}^3 \left(\frac{1}{m_n(i)} - \frac{1}{m_n(f)} \right) m_n(i) u_{nu}(ks) u_{nu}(lt) \frac{\partial}{\partial Q_{ks}} \frac{\partial}{\partial Q_{lt}} = \\
&= \frac{1}{2} \sum_{n=1}^K \sum_{u=1}^3 \sum_{k=1}^N \sum_{s=1}^3 \sum_{l=1}^N \sum_{t=1}^3 \left(1 - \frac{m_n(i)}{m_n(f)} \right) u_{nu}(ks) u_{nu}(lt) \frac{\partial}{\partial Q_{ks}} \frac{\partial}{\partial Q_{lt}} \tag{B.7}
\end{aligned}$$

The expression above can be simplified by introducing combined indices to label the normal modes, as well as by introducing vector notation for the atomic normal mode displacements:

$$W(i \rightarrow f) = \sum_{n=1}^K W_n(i \rightarrow f) = \frac{1}{2} \sum_{n=1}^K \sum_{r=1}^{3N} \sum_{s=1}^{3N} \left(1 - \frac{m_n(i)}{m_n(f)} \right) \bar{u}(r)_n \bar{u}(s)_n \frac{\partial}{\partial Q_r} \frac{\partial}{\partial Q_s} \tag{B.8}$$

Since the momentum representation of the momentum operator is given by:

$$\hat{P}_r = -i \frac{\partial}{\partial Q_r} \tag{B.9}$$

and recalling that the momentum operator was quantized in Eq. (B.2) in terms of the ladder operators:

$$\begin{aligned}
\hat{Q}_r &= \sqrt{\frac{1}{2\omega_r}} (a_r^\dagger + a_r) \\
\hat{P}_r &= i \sqrt{\frac{\omega_r}{2}} (a_r^\dagger - a_r) \tag{B.10}
\end{aligned}$$

we have,

$$\hat{P}_r = -i \frac{\partial}{\partial Q_r} = i \sqrt{\frac{\omega_r}{2}} (a_r^\dagger - a_r) \tag{B.11}$$

so that:

$$\frac{\partial}{\partial Q_r} = -\sqrt{\frac{\omega_r}{2}} (a_r^\dagger - a_r) \quad (\text{B.12})$$

Inserting this in the expression for the isotopic perturbation (B.8):

$$\begin{aligned} W(i \rightarrow f) &= \sum_{n=1}^K W_n(i \rightarrow f) = \\ &= \frac{1}{2} \sum_{n=1}^K \sum_{r=1}^{3N} \sum_{s=1}^{3N} \left(1 - \frac{m_n(i)}{m_n(f)} \right) \bar{u}(r)_n \bar{u}(s)_n \left(-\sqrt{\frac{\omega_r}{2}} (a_r^\dagger - a_r) \right) \left(-\sqrt{\frac{\omega_s}{2}} (a_s^\dagger - a_s) \right) = \\ &= \frac{1}{4} \sum_{n=1}^K \sum_{r=1}^{3N} \sum_{s=1}^{3N} \left(1 - \frac{m_n(i)}{m_n(f)} \right) \bar{u}_n(r) \bar{u}_n(s) (a_r^\dagger - a_r) (a_s^\dagger - a_s) \sqrt{\omega_r} \sqrt{\omega_s} \end{aligned} \quad (\text{B.13})$$

Thus, the perturbation has been written in terms of the ladder operators.

As it will be noticed in Appendices B and C, introducing the normal ordered operators H_N and $W_N[K]$ will simplify the derivations of the first and second order corrections in non-degenerate perturbation theory to the isotopic shifts. Any string of ladder operators written in normal order is such that all creation operators are placed to the left of all annihilation operators. Thus, by normal ordering with respect to the vibrational ground state, the unperturbed Hamiltonian (B.4) can be written as:

$$H_0 = H_N + E_0 \quad (\text{B.14})$$

with

$$\begin{aligned} H_N &= \sum_{r=1}^M \omega_r \{ a_r^\dagger a_r \} = \sum_{r=1}^M \omega_r a_r^\dagger a_r \\ E_0 &= \frac{1}{2} \sum_{r=1}^M \omega_r \end{aligned} \quad (\text{B.15})$$

such that

$$\langle 0 | H_N | 0 \rangle = 0$$

Furthermore, by writing the isotopic perturbation as:

$$\begin{aligned}
W[K](i \rightarrow f) &= \sum_{rs=1}^M \sum_{n=1}^K \lambda_n V_{n,rs} (a_r^\dagger - a_r)(a_s^\dagger - a_s) \\
V_{n,rs} &= \frac{\sqrt{\omega_r} \sqrt{\omega_s}}{4} \bar{u}_n(r) \bar{u}_n(s) \\
\lambda_n &= \left(1 - \frac{m_n(i)}{m_n(f)} \right)
\end{aligned} \tag{B.16}$$

the perturbation can be written as:

$$W[K](i \rightarrow f) = W_N[K] - \sum_{r=1}^M \sum_{n=1}^K \lambda_n V_{n,rr} \tag{B.17}$$

where $W_N[K]$ is the normal order perturbation:

$$\begin{aligned}
W_N[K] &= \sum_{rs}^M \sum_{n=1}^K \lambda_n V_{n,rs} \left(\{a_r a_s\} - \{a_r^\dagger a_s\} - \{a_r a_s^\dagger\} + \{a_r^\dagger a_s^\dagger\} \right) = \\
& \sum_{rs}^M \sum_{n=1}^K \lambda_n V_{n,rs} \left(a_r a_s - 2a_r^\dagger a_s + a_r^\dagger a_s^\dagger \right)
\end{aligned} \tag{B.18}$$

The expressions (B.14) and (B.17) written in terms of normal ordered operators will be used in Appendices C and D in order to simplify the derivations of the first and second order corrections to the isotopic shifts.

C. Derivation of the First Order Correction to an Isotopic Shift³⁹

The first order correction to the energy shift for the state Ψ in non-degenerate perturbation theory is given by:

$$\Delta E[K] = \langle \Psi | W[K](i \rightarrow f) | \Psi \rangle \quad (\text{C.1})$$

A fundamental absorption is obtained experimentally when a transition from the ground state to a single excited vibrational state occurs, this is:

$$|0\rangle \rightarrow |\Psi_t\rangle = a_t^\dagger |0\rangle \quad (\text{C.2})$$

Therefore, the first order frequency shift of the vibrational fundamental absorption due to an isotopic mass perturbation is given by:

$$\Delta \omega_t^{(1)}[K] = \langle \Psi_t | W[K](i \rightarrow f) | \Psi_t \rangle - \langle 0 | W[K](i \rightarrow f) | 0 \rangle \quad (\text{C.3})$$

Using the normal ordered operator (B.17) to simplify the evaluation of the last equation, we have:

$$\begin{aligned} \Delta \omega_t^{(1)}[K] &= \langle \Psi_t | W[K](i \rightarrow f) | \Psi_t \rangle - \langle 0 | W[K](i \rightarrow f) | 0 \rangle = \\ &= \left\langle \Psi_t \left| W_N[K] - \sum_r \sum_{n=1}^K \lambda_n V_{n,rr} \right| \Psi_t \right\rangle - \left\langle 0 \left| W_N[K] - \sum_r \sum_{n=1}^K \lambda_n V_{n,rr} \right| 0 \right\rangle = \\ &= \langle \Psi_t | W_N[K] | \Psi_t \rangle - \langle 0 | W_N[K] | 0 \rangle = \langle \Psi_t | W_N[K] | \Psi_t \rangle \end{aligned} \quad (\text{C.4})$$

Evaluating this matrix element we have:

$$\begin{aligned} \langle \Psi_t | W_N[K] | \Psi_t \rangle &= \sum_{rs} \sum_{n=1}^K \lambda_n V_{n,rs} \langle 0 | a_t (a_r a_s - 2a_r^\dagger a_s + a_r^\dagger a_s^\dagger) a_t^\dagger | 0 \rangle = \\ &= -2 \sum_{rs} \sum_{n=1}^K \lambda_n V_{n,rs} \langle 0 | a_t a_r^\dagger a_s a_t^\dagger | 0 \rangle = -2 \sum_{n=1}^K \lambda_n V_{n,tt} \end{aligned} \quad (\text{C.5})$$

Recalling from the group of equations (B.16), $V_{n,rs}$ and λ_n were defined as:

$$V_{n,rs} = \frac{\sqrt{\omega_r} \sqrt{\omega_s}}{4} \vec{u}_n(r) \vec{u}_n(s)$$

$$\lambda_n = \left(1 - \frac{m_n(i)}{m_n(f)} \right)$$

Therefore, to first order in non-degenerate perturbation theory the frequency shift caused by an isotopic perturbation is given by:

$$\Delta\omega_i^{(1)}[K](i \rightarrow f) = -\frac{\omega_i}{2} \sum_{n=1}^K \left(1 - \frac{m_n(i)}{m_n(f)} \right) |\vec{u}_n(t)|^2 \quad (\text{C.6})$$

D. Derivation of the Second Order Correction to an Isotopic Shift³⁹

The second order correction to the energy in non-degenerate perturbation theory is given by:

$$E^{(2)}[K] = \sum_{\alpha \neq \beta} \frac{|\langle \alpha | W[K](i \rightarrow f) | \beta \rangle|^2}{E_\alpha - E_\beta} \quad (\text{D.1})$$

where $W[K](i \rightarrow f)$ is the isotopic mass perturbation given by Eq. (B.17).

The second order energy shift in a transition from the ground state to a single excited vibrational state t is given by:

$$\Delta E^{(2)}[K] = E_t^{(2)}[K] - E_0^{(2)}[K] \quad (\text{D.2})$$

In order to evaluate Eq. (D.2), the second order corrections $E_0^{(2)}[K]$ and $E_t^{(2)}[K]$ will be evaluated separately.

The second order correction to the ground state energy is given by:

$$E_0^{(2)}[K] = \sum_{0 \neq \beta} \frac{|\langle 0 | W[K](i \rightarrow f) | \beta \rangle|^2}{E_0 - E_\beta} = \sum_{0 \neq \beta} \frac{\left| \langle 0 | W_N[K] - \sum_r \sum_{n=1}^K \lambda_n V_{n,rr} | \beta \rangle \right|^2}{E_0 - E_\beta} = \sum_{0 \neq \beta} \frac{|\langle 0 | W_N[K] | \beta \rangle|^2}{E_0 - E_\beta} \quad (\text{D.3})$$

where $V_{n,rs}$ and λ_n have been defined as:

$$V_{n,rs} = \frac{\sqrt{\omega_r} \sqrt{\omega_s}}{4} \bar{u}_n(r) \bar{u}_n(s)$$

$$\lambda_n = \left(1 - \frac{m_n(i)}{m_n(f)} \right)$$

Since only one term of the normal ordered perturbation $W_N[K]$ survives, we have:

$$E_0^{(2)} [K] = \sum_{0 \neq \beta} \frac{\left| \sum_{rs} \sum_{n=1}^K \lambda_n V_{n,rs} \langle 0 | a_r a_s | \beta \rangle \right|^2}{E_0 - E_\beta} \quad (\text{D.4})$$

In order to ensure proper normalization of the possible excited states, two possibilities are identified:

$$|\beta\rangle = \begin{cases} a_u^\dagger a_v^\dagger |0\rangle & ; u \neq v \\ \frac{1}{\sqrt{2}} a_u^\dagger a_u^\dagger |0\rangle \end{cases} \quad (\text{D.5})$$

This gives us:

$$E_0^{(2)} [K] = \frac{1}{2} \sum_{u \neq v} \frac{\left| \sum_{rs} \sum_{n=1}^K \lambda_n V_{n,rs} \langle 0 | a_r a_s a_u^\dagger a_v^\dagger |0\rangle \right|^2}{E_0 - E_{uv}} + \sum_u \frac{\left| \sum_{rs} \sum_{n=1}^K \lambda_n V_{n,rs} \langle 0 | a_r a_s \frac{1}{\sqrt{2}} a_u^\dagger a_u^\dagger |0\rangle \right|^2}{E_0 - E_{uu}} \quad (\text{D.6})$$

The factor of $\frac{1}{2}$ in the first term is necessary to avoid double counting the states $a_u^\dagger a_v^\dagger |0\rangle$ and $a_v^\dagger a_u^\dagger |0\rangle$. Equation (D.6) simplifies to:

$$E_0^{(2)} [K] = \frac{1}{2} \sum_{uv} \frac{\left| \sum_{rs} \sum_{n=1}^K \lambda_n V_{n,rs} \langle 0 | a_r a_s a_u^\dagger a_v^\dagger |0\rangle \right|^2}{E_0 - E_{uv}} \quad (\text{D.7})$$

Evaluating the operator product we find:

$$\begin{aligned}
\langle 0|a_r a_s a_u^\dagger a_v^\dagger|0\rangle &= \langle 0|a_r (\delta_{us} + a_u^\dagger a_s) a_v^\dagger|0\rangle = \\
&\delta_{us} \langle 0|a_r a_v^\dagger|0\rangle + \langle 0|a_r a_u^\dagger a_s a_v^\dagger|0\rangle = \\
&\delta_{us} \langle 0|(\delta_{rv} + a_v^\dagger a_r)|0\rangle + \langle 0|a_r a_u^\dagger (\delta_{sv} + a_v^\dagger a_s)|0\rangle = \\
&\delta_{us} \delta_{rv} + \delta_{sv} \langle 0|a_r a_u^\dagger|0\rangle = \delta_{us} \delta_{rv} + \delta_{sv} \langle 0|(\delta_{ru} + a_u^\dagger a_r)|0\rangle = \\
&\delta_{us} \delta_{rv} + \delta_{sv} \delta_{ru}
\end{aligned} \tag{D.8}$$

Therefore,

$$\begin{aligned}
E_0^{(2)}[K] &= \frac{1}{2} \sum_{uv} \frac{\left| \sum_{rs} \sum_{n=1}^K \lambda_n V_{n,rs} (\delta_{us} \delta_{rv} + \delta_{sv} \delta_{ru}) \right|^2}{E_0 - E_{uv}} = \\
&\frac{1}{2} \sum_{uv} \frac{\left| \sum_{rs} \sum_{n=1}^K \lambda_n V_{n,rs} \delta_{us} \delta_{rv} + \sum_{rs} \sum_{n=1}^K \lambda_n V_{n,rs} \delta_{sv} \delta_{ru} \right|^2}{E_0 - (E_0 + \omega_u + \omega_v)} = \\
&\frac{1}{2} \sum_{uv} \frac{\left| \sum_{n=1}^K \lambda_n V_{n,vu} + \sum_{n=1}^K \lambda_n V_{n,uv} \right|^2}{E_0 - (E_0 + \omega_u + \omega_v)} = -2 \sum_{uv} \frac{\left| \sum_{n=1}^K \lambda_n V_{n,uv} \right|^2}{\omega_u + \omega_v}
\end{aligned} \tag{D.9}$$

This result represents the second order correction to the ground state energy.

In order to evaluate the second order correction to the singly excited state $E_t^{(2)}[K]$,

we first define:

$$|\Psi_t\rangle = |t\rangle = a_t^\dagger |0\rangle \tag{D.10}$$

Thus, we can write:

$$\begin{aligned}
E_t^{(2)}[K] &= \sum_{t \neq \beta} \frac{|\langle t|W[K](i \rightarrow f)|\beta\rangle|^2}{E_0 - E_\beta} = \sum_{t \neq \beta} \frac{\left| \langle t|W_N[K] - \sum_r \sum_{n=1}^K \lambda_n V_{n,rr} |\beta\rangle \right|^2}{E_t - E_\beta} = \\
&\sum_{t \neq \beta} \frac{|\langle t|W_N[K]|\beta\rangle|^2}{E_t - E_\beta} = \sum_{t \neq \beta} \frac{\left| \langle 0|a_t \sum_{rs} \sum_{n=1}^K \lambda_n V_{n,rs} (a_r a_s - 2a_r^\dagger a_s + a_r^\dagger a_s^\dagger) |\beta\rangle \right|^2}{E_t - E_\beta}
\end{aligned} \tag{D.11}$$

There can be no contribution from the $a_r^\dagger a_s^\dagger$ part of the perturbation since any state formed from this operator would be orthogonal to the excited state we are considering.

Consequently,

$$E_t^{(2)} [K] = \sum_{t \neq \beta} \frac{\left| \sum_{rs} \sum_{n=1}^K \lambda_n V_{n,rs} \langle 0 | a_t (a_r a_s - 2a_r^\dagger a_s) | \beta \rangle \right|^2}{E_t - E_\beta} =$$

$$\sum_{t \neq \beta} \frac{\left| \sum_{rs} \sum_{n=1}^K \lambda_n V_{n,rs} \langle 0 | a_t a_r a_s | \beta \rangle \right|^2}{E_t - E_\beta} + 4 \sum_{t \neq \beta} \frac{\left| \sum_{rs} \sum_{n=1}^K \lambda_n V_{n,rs} \langle 0 | a_t a_r^\dagger a_s | \beta \rangle \right|^2}{E_t - E_\beta} \quad (\text{D.12})$$

The terms in Eq. (D.12) also need to be evaluated separately. Starting with the second term we find:

$$4 \sum_{t \neq \beta} \frac{\left| \sum_{rs} \sum_{n=1}^K \lambda_n V_{n,rs} \langle 0 | a_t a_r^\dagger a_s | \beta \rangle \right|^2}{E_t - E_\beta} = 4 \sum_{t \neq u} \frac{\left| \sum_{rs} \sum_{n=1}^K \lambda_n V_{n,rs} \langle 0 | a_t a_r^\dagger a_s a_u^\dagger | 0 \rangle \right|^2}{\omega_t - \omega_u} =$$

$$4 \sum_{t \neq u} \frac{\left| \sum_{rs} \sum_{n=1}^K \lambda_n V_{n,rs} \langle 0 | \delta_{tr} \delta_{su} | 0 \rangle \right|^2}{\omega_t - \omega_u} = 4 \sum_{t \neq u} \frac{\left| \sum_{n=1}^K \lambda_n V_{n,tu} \right|^2}{\omega_t - \omega_u} \quad (\text{D.13})$$

The first term is more complicated. The excited state $|\beta\rangle$ can now be of the form:

$$|\beta\rangle = \frac{1}{\sqrt{K}} a_u^\dagger a_v^\dagger a_y^\dagger |0\rangle \quad (\text{D.14})$$

where at least one of the indices u, v, y has to equal t in order to get a non-zero contribution. Thus, the first term of Eq. (D.12) is:

$$\begin{aligned}
& \sum_{t \neq \beta} \frac{\left| \sum_{rs} \sum_{n=1}^K \lambda_n V_{n,rs} \langle 0 | a_t a_r a_s | \beta \rangle \right|^2}{E_t - E_\beta} = \\
& \sum_{u \neq t} \frac{\left| \sum_{rs} \sum_{n=1}^K \lambda_n V_{n,rs} \langle 0 | a_t a_r a_s \frac{1}{\sqrt{2}} a_u^\dagger a_u^\dagger a_t^\dagger | 0 \rangle \right|^2}{\omega_t - (2\omega_u + \omega_t)} + \\
& \frac{1}{2} \sum_{\substack{u \neq v \neq t \\ uv \neq t}} \frac{\left| \sum_{rs} \sum_{n=1}^K \lambda_n V_{n,rs} \langle 0 | a_t a_r a_s a_u^\dagger a_v^\dagger a_t^\dagger | 0 \rangle \right|^2}{\omega_t - (\omega_u + \omega_v + \omega_t)} \\
& + \frac{\left| \sum_{rs} \sum_{n=1}^K \lambda_n V_{n,rs} \langle 0 | a_t a_r a_s \frac{1}{\sqrt{6}} a_t^\dagger a_t^\dagger a_t^\dagger | 0 \rangle \right|^2}{\omega_t - (2\omega_t + \omega_t)} + \\
& \sum_{u \neq v = t} \frac{\left| \sum_{rs} \sum_{n=1}^K \lambda_n V_{n,rs} \langle 0 | a_t a_r a_s \frac{1}{\sqrt{2}} a_u^\dagger a_t^\dagger a_t^\dagger | 0 \rangle \right|^2}{\omega_t - (\omega_u + \omega_t + \omega_t)} = \\
& - \frac{1}{4} \sum_{u \neq t} \frac{\left| \sum_{rs} \sum_{n=1}^K \lambda_n V_{n,rs} \langle 0 | a_t a_r a_s a_u^\dagger a_u^\dagger a_t^\dagger | 0 \rangle \right|^2}{\omega_u} \\
& \frac{1}{2} \sum_{\substack{u \neq v \neq t \\ uv \neq t}} \frac{\left| \sum_{rs} \sum_{n=1}^K \lambda_n V_{n,rs} \langle 0 | a_t a_r a_s a_u^\dagger a_v^\dagger a_t^\dagger | 0 \rangle \right|^2}{\omega_u + \omega_v} \\
& - \frac{1}{6} \frac{\left| \sum_{rs} \sum_{n=1}^K \lambda_n V_{n,rs} \langle 0 | a_t a_r a_s a_t^\dagger a_t^\dagger a_t^\dagger | 0 \rangle \right|^2}{2\omega_t} \\
& \frac{1}{2} \sum_{u \neq t} \frac{\left| \sum_{rs} \sum_{n=1}^K \lambda_n V_{n,rs} \langle 0 | a_t a_r a_s a_u^\dagger a_t^\dagger a_t^\dagger | 0 \rangle \right|^2}{\omega_u + \omega_t} \tag{D.15}
\end{aligned}$$

Evaluating the matrix elements forming all possible contractions between the creation and annihilation operators in Eq. (D.15), we have:

$$\begin{aligned}
\langle 0 | a_t a_r a_s a_u^\dagger a_u^\dagger a_t^\dagger | 0 \rangle &= 2 \delta_{su} \delta_{ru} \\
\langle 0 | a_t a_r a_s a_u^\dagger a_v^\dagger a_t^\dagger | 0 \rangle &= 2 \delta_{su} \delta_{rv} \\
\langle 0 | a_t a_r a_s a_t^\dagger a_t^\dagger a_t^\dagger | 0 \rangle &= 6 \delta_{rt} \delta_{st} \\
\langle 0 | a_t a_r a_s a_u^\dagger a_t^\dagger a_t^\dagger | 0 \rangle &= 4 \delta_{su} \delta_{rt}
\end{aligned} \tag{D.16}$$

Thus, the first term in Eq. (D.12) takes the form:

$$\begin{aligned}
\sum_{t \neq \beta} \frac{\left| \sum_{rs} \sum_{n=1}^K \lambda_n V_{n,rs} \langle 0 | a_t a_r a_s | \beta \rangle \right|^2}{E_t - E_\beta} &= -\frac{1}{4} \sum_{u \neq t} \frac{\left| \sum_{n=1}^K \lambda_n V_{n,uu} \right|^2}{\omega_u} \times 4 - \\
\frac{1}{2} \sum_{\substack{u \neq v \neq t \\ uv \neq t}} \frac{\left| \sum_{n=1}^K \lambda_n V_{n,vu} \right|^2}{\omega_u + \omega_v} \times 4 &- \frac{1}{6} \frac{\left| \sum_{n=1}^K \lambda_n V_{n,tt} \right|^2}{2\omega_t} \times 36 - \frac{1}{2} \sum_{u \neq t} \frac{\left| \sum_{n=1}^K \lambda_n V_{n,ut} \right|^2}{\omega_u + \omega_t} \times 16
\end{aligned} \tag{D.17}$$

The results found in Eq. (D.13) and Eq. (D.17) provide the second order correction

$E_t^{(2)}[K]$:

$$\begin{aligned}
E_t^{(2)}[K] &= 4 \sum_{t \neq u} \frac{\left| \sum_{n=1}^K \lambda_n V_{n,tu} \right|^2}{\omega_t - \omega_u} - \sum_{u \neq t} \frac{\left| \sum_{n=1}^K \lambda_n V_{n,uu} \right|^2}{\omega_u} - 2 \sum_{\substack{u \neq v \neq t \\ uv \neq t}} \frac{\left| \sum_{n=1}^K \lambda_n V_{n,vu} \right|^2}{\omega_u + \omega_v} - \\
3 \frac{\left| \sum_{n=1}^K \lambda_n V_{n,tt} \right|^2}{\omega_t} &- 8 \sum_{u \neq t} \frac{\left| \sum_{n=1}^K \lambda_n V_{n,ut} \right|^2}{\omega_u + \omega_t}
\end{aligned} \tag{D.18}$$

and the second order energy shift for the particular state becomes:

$$\begin{aligned}
\Delta E^{(2)}[K] &= E_t^{(2)}[K] - E_0^{(2)}[K] = \\
&4 \sum_{u \neq t} \frac{\left| \sum_{n=1}^K \lambda_n V_{n,tu} \right|^2}{\omega_t - \omega_u} - \sum_{u \neq t} \frac{\left| \sum_{n=1}^K \lambda_n V_{n,uu} \right|^2}{\omega_u} - 2 \sum_{\substack{u \neq v \neq t \\ uv \neq t}} \frac{\left| \sum_{n=1}^K \lambda_n V_{n,vu} \right|^2}{\omega_u + \omega_v} \\
&3 \frac{\left| \sum_{n=1}^K \lambda_n V_{n,tt} \right|^2}{\omega_t} - 8 \sum_{u \neq t} \frac{\left| \sum_{n=1}^K \lambda_n V_{n,ut} \right|^2}{\omega_u + \omega_t} + 2 \sum_{uv} \frac{\left| \sum_{n=1}^K \lambda_n V_{n,uv} \right|^2}{\omega_u + \omega_v}
\end{aligned} \tag{D.19}$$

Finally, by splitting the last term in Eq. (D.19), originating from the ground state correction

(D.9), the second order energy shift $\Delta E^{(2)}[K]$ can be written as:

$$\begin{aligned}
\Delta E^{(2)}[K] &= \\
&4 \sum_{u \neq t} \frac{\left| \sum_{n=1}^K \lambda_n V_{n,tu} \right|^2}{\omega_t - \omega_u} - \sum_{u \neq t} \frac{\left| \sum_{n=1}^K \lambda_n V_{n,uu} \right|^2}{\omega_u} - 2 \sum_{\substack{u \neq v \neq t \\ uv \neq t}} \frac{\left| \sum_{n=1}^K \lambda_n V_{n,vu} \right|^2}{\omega_u + \omega_v} - 3 \frac{\left| \sum_{n=1}^K \lambda_n V_{n,tt} \right|^2}{\omega_t} \\
&8 \sum_{u \neq t} \frac{\left| \sum_{n=1}^K \lambda_n V_{n,ut} \right|^2}{\omega_u + \omega_t} + 2 \sum_{\substack{u \neq v \neq t \\ uv \neq t}} \frac{\left| \sum_{n=1}^K \lambda_n V_{n,uv} \right|^2}{\omega_u + \omega_v} + 2 \sum_{u \neq t} \frac{\left| \sum_{n=1}^K \lambda_n V_{n,ut} \right|^2}{\omega_u + \omega_t} \times 2 + \\
&\sum_{u \neq t} \frac{\left| \sum_{n=1}^K \lambda_n V_{n,uu} \right|^2}{\omega_u} + \frac{\left| \sum_{n=1}^K \lambda_n V_{n,tt} \right|^2}{\omega_t} = 4 \left(\sum_{u \neq t} \frac{\left| \sum_{n=1}^K \lambda_n V_{n,tu} \right|^2}{\omega_t - \omega_u} - \sum_u \frac{\left| \sum_{n=1}^K \lambda_n V_{n,ut} \right|^2}{\omega_u + \omega_t} \right)
\end{aligned} \tag{D.20}$$

E. Bracketing Theorem

A convenient way to generate the terms of Rayleigh-Schrödinger perturbation theory (RSPT) is given by the bracketing theorem.⁶²

With the following definitions:

$$\begin{aligned} \langle W \rangle &= \langle n | W | n \rangle \\ R &= \sum_{m \neq n} \frac{|m\rangle \langle m|}{E_n^{(0)} - E_m^{(0)}} \end{aligned} \quad (\text{E.1})$$

the corrections to the energy in RSPT are given by:

$$\begin{aligned} E_n^{(0)} &= E_n^{(0)} \\ E_n^{(1)} &= \langle W \rangle \\ E_n^{(2)} &= \langle WRW \rangle \\ E_n^{(3)} &= \langle W (RW)^2 \rangle - \langle W \rangle \langle WR^2W \rangle \\ E_n^{(4)} &= \langle W (RW)^3 \rangle - \langle W \rangle \left(\langle WR(RW)^2 \rangle + \langle (WR)^2 RW \rangle \right) + \\ &\quad \langle W \rangle^2 \langle WR^3W \rangle - \langle WRW \rangle \langle WR^2W \rangle \\ &\quad \vdots \end{aligned} \quad (\text{E.2})$$

The general expression has the form:

$$E^{(k)} = \langle W (RW)^{k-1} \rangle + \mathfrak{R}^{(k)} \quad (\text{E.3})$$

The first term of the Eq. (E.3) is referred to as the principal k th order term, while the terms included in $\mathfrak{R}^{(k)}$ are referred to as the renormalization terms that are obtained through the application of the following rules:

1. Insert the bracketings $\langle \dots \rangle$ around the $W, WRW, \dots, WR \cdots RW$ operator strings of the principal term in all possible ways.
2. Bracketings involving the rightmost and/or the leftmost interactions vanish.

3. The sign of each bracketed term is given by $(-1)^{n_B}$, where n_B is the number of bracketings.

4. Bracketings within bracketings are allowed, e.g.,

$$\langle WR \langle WR \langle W \rangle RW \rangle RW \rangle = \langle W \rangle \langle WR^2 W \rangle^2$$

5. The total number of bracketings (including the principal terms) is

$$(2k-2)! / [k!(k-1)!].$$

Thus, the explicit form of the terms in Eq. (E.2) is given by:

$$\begin{aligned}
E_n^{(0)} &= E_n^{(0)} \\
E_n^{(1)} &= \langle W \rangle = \langle n|W|n \rangle \\
E_n^{(2)} &= \langle WRW \rangle = \sum_{m \neq n} \frac{\langle n|W|m \rangle \langle m|W|n \rangle}{E_n^{(0)} - E_m^{(0)}} \\
E_n^{(3)} &= \langle W(RW)^2 \rangle - \langle W \rangle \langle WR^2 W \rangle = \sum_{l \neq n} \sum_{m \neq n} \frac{\langle n|W|m \rangle \langle m|W|l \rangle \langle l|W|n \rangle}{(E_n^{(0)} - E_m^{(0)})(E_n^{(0)} - E_l^{(0)})} - \\
&\langle n|W|n \rangle \sum_{m \neq n} \frac{\langle n|W|m \rangle \langle m|W|n \rangle}{(E_n^{(0)} - E_m^{(0)})^2}
\end{aligned} \tag{E.4}$$

References

- ¹ J. Simons, *J. Phys. Chem.* **95**, 1017 (1991).
- ² A. Szabo, N.S. Ostlund, *Modern Quantum Chemistry: introduction to advanced electronic structure theory*, (Dover, New York, 1996).
- ³ M. Head-Gordon, E. Artacho, *Physics Today*, 58 (April 2008).
- ⁴ M. Born, R. Oppenheimer, *Ann. Phys.* **84**, 457 (1927).
- ⁵ D. A. Yarkony, *Atomic Molecular and Optical Physics Handbook*, Editor: G. W. F. Drake, (American Institute of Physics Press, 1996).
- ⁶ H. A. Bethe and E. E. Salpeter, *Quantum Mechanics of One and Two Electron Atoms*, (Plenum/Rosetta, New York, 1977).
- ⁷ D. W. Jepsen, J. O. Hirschfelder, *J. Chem. Phys.* **32**, 1323 (1960).
- ⁸ J. B. Foresman, A. Frisch, *Exploring Chemistry with Electronic Structure Methods*, 2nd Ed., (Gaussian Inc., Pittsburgh, PA, 1996).
- ⁹ D. M. Bishop, *Group Theory and Chemistry*, (Dover, New York, 1993).
- ¹⁰ C. M. L. Rittby, *J. Chem. Phys.* **95**, 5609 (1991).
- ¹¹ C. M. L. Rittby, *J. Chem. Phys.* **96**, 6768 (1992).
- ¹² E. B. Wilson, J. C. Decius, and P. C. Cross, *Molecular Vibrations*, (McGraw-Hill, New York, 1955).
- ¹³ G. Herzberg, *Infrared and Raman Spectra*, (Van Nostrand, New York, 1945).
- ¹⁴ S. Maeda, Y. Watanabe, and K. Ohno, *J. Chem. Phys.* **128**, 144111 (2008).
- ¹⁵ Y. Scribano, and D. M. Benoit, *J. Chem. Phys.* **127**, 164118 (2007).

-
- ¹⁶ D. A. Clabo, W. D. Allen, R. B. Remington, Y. Yamaguchi, and H. F. Schaefer III, *Chem. Phys.* **123**, 187 (1988).
- ¹⁷ R. Burcl, N. C. Handy, and S. Carter, *Spectrochim. Acta, Part A* **59**, 1881 (2003).
- ¹⁸ V. Barone, *J. Chem. Phys.* **122**, 014108 (2005).
- ¹⁹ J. D. Presilla-Márquez, S. C. Gay, C. M. L. Rittby, and W. R. M. Graham, *J. Chem. Phys.* **102**, 6354 (1995).
- ²⁰ S. A. Bates, C. M. L. Rittby, and W. R. M. Graham, *J. Chem. Phys.* **128**, 234301 (2008).
- ²¹ R. E. Kinzer, Jr., C. M. L. Rittby, and W. R. M. Graham, *J. Chem. Phys.* **128**, 64312(2008).
- ²² E. Gonzalez, C. M. L. Rittby, and W. R. M. Graham, *J. Chem. Phys.* **125**, 44504 (2006).
- ²³ D. S. Han, C. M. L. Rittby, and W. R. M. Graham, *J. Chem. Phys.* **109**, 8355 (1998).
- ²⁴ X. D. Ding, S. L. Wang, C. M. L. Rittby, and W. R. M. Graham, *J. Phys. Chem. A.* **104**, 3712 (2000).
- ²⁵ Q. Jiang, C. M. L. Rittby, and W. R. M. Graham, *J. Chem. Phys.* **99**, 3194 (1993).
- ²⁶ L. N. Shen and W. R. M. Graham, *J. Chem. Phys.* **91**, 5115 (1989).
- ²⁷ R. H. Kranze and W. R. M. Graham, *J. Chem. Phys.* **96**, 2517 (1992).
- ²⁸ R. H. Kranze and W. R. M. Graham, *J. Chem. Phys.* **98**, 71 (1993).
- ²⁹ R. H. Kranze, P. A. Withey, C. M. L. Rittby, and W. R. M. Graham, *J. Chem. Phys.* **103**, 6841 (1995).
- ³⁰ R. H. Kranze, C. M. L. Rittby, and W. R. M. Graham, *J. Chem. Phys.* **105**, 5313 (1996).
- ³¹ X. D. Ding, S. L. Wang, C. M. L. Rittby, and W. R. M. Graham, *J. Chem. Phys.* **112**, 5113 (2000).
- ³² S. L. Wang, C. M. L. Rittby, and W. R. M. Graham, *J. Chem. Phys.* **107**, 6032 (1997).

-
- ³³ S. L. Wang, C. M. L. Rittby, and W. R. M. Graham, *J. Chem. Phys.* **107**, 7025 (1997).
- ³⁴ W. Weltner, Jr., and R. J. Van Zee, *Chem. Rev.* **89**, 1713 (1989).
- ³⁵ S. Yang and M. Kertesz, *J. Phys. Chem. A* **112**, 146 (2008).
- ³⁶ S. Arulmozhiraja and T. Ohno, *J. Chem. Phys.* **128**, 114301 (2008).
- ³⁷ J. Hunter, J. Fye, and M. F. Jarrold, *J. Chem. Phys.* **99**, 1785 (1993).
- ³⁸ G. V. Helden, N. G. Gotts, and M. T. Bowers, *J. Am. Chem. Soc.* **115**, 4363 (1993).
- ³⁹ C. M. L. Rittby (unpublished work).
- ⁴⁰ R. Cárdenas, *Infrared Studies of the Spectra and Structures of Novel Carbon Clusters*, Ph.D. Thesis, Texas Christian University (2007).
- ⁴¹ C. Cohen-Tannoudji, B. Diu, F. Laloë, *Quantum Mechanics Volume Two*, (Wiley-Interscience, New York, 1977).
- ⁴² A. M. Kosevich, *The Crystal Lattice: Phonons, Solitons, Dislocations, Superlattices, Second Edition*, (Wiley-VCH, Weinheim, 2005).
- ⁴³ G. García, *Predissertation* (2007).
- ⁴⁴ Gaussian 03, Revision E.01, M. J. Frisch, G. W. Trucks, H. B. Schlegel, G. E. Scuseria, M. A. Robb, J. R. Cheeseman, J. A. Montgomery, Jr., T. Vreven, K. N. Kudin, J. C. Burant, J. M. Millam, S. S. Iyengar, J. Tomasi, V. Barone, B. Mennucci, M. Cossi, G. Scalmani, N. Rega, G. A. Petersson, H. Nakatsuji, M. Hada, M. Ehara, K. Toyota, R. Fukuda, J. Hasegawa, M. Ishida, T. Nakajima, Y. Honda, O. Kitao, H. Nakai, M. Klene, X. Li, J. E. Knox, H. P. Hratchian, J. B. Cross, V. Bakken, C. Adamo, J. Jaramillo, R. Gomperts, R. E. Stratmann, O. Yazyev, A. J. Austin, R. Cammi, C. Pomelli, J. W. Ochterski, P. Y. Ayala, K. Morokuma, G. A. Voth, P. Salvador, J. J. Dannenberg, V. G. Zakrzewski, S. Dapprich, A. D. Daniels, M. C. Strain, O. Farkas, D. K. Malick, A. D. Rabuck, K. Raghavachari, J. B. Foresman, J. V. Ortiz, Q. Cui, A. G. Baboul, S. Clifford, J. Cioslowski, B. B. Stefanov, G. Liu, A. Liashenko, P. Piskorz, I. Komaromi, R. L. Martin, D. J. Fox, T. Keith, M. A. Al-Laham, C. Y. Peng, A. Nanayakkara, M. Challacombe, P. M. W. Gill, B. Johnson, W. Chen, M. W. Wong, C. Gonzalez, and J. A. Pople, Gaussian, Inc., Wallingford CT, 2004.

-
- ⁴⁵ M. E. Jacox, NIST Vibrational and Electronic Energy Levels Database, (<http://webbook.nist.gov/chemistry>).
- ⁴⁶ J. Szczepanski, S. Ekern, C. Chapo, and M. Vala, Chem. Phys. **211**, 359 (1996).
- ⁴⁷ J. F. Fuller, J. Szczepanski, and M. Vala, Chem. Phys. Lett. **323**, 86 (2000).
- ⁴⁸ J. M. L. Martin and P. R. Taylor, J. Phys. Chem. **98**, 6105 (1994).
- ⁴⁹ J. M. L. Martin, D. W. Schwenke, T. J. Lee, and P. R. Taylor, J. Chem. Phys. **104**, 4657 (1996).
- ⁵⁰ H. Massó, V. Veryazov, P.-Å. Malmqvist, and B. O. Roos, J. Chem. Phys. **127**, 154318 (2007).
- ⁵¹ P. Botschwina and P. Sebald, Chem. Phys. Lett. **160**, 485 (1989).
- ⁵² M. Mladenović, S. Schmatz, and P. Botschwina, J. Chem. Phys. **101**, 5891 (1994).
- ⁵³ P. Botschwina, J. Phys. Chem. A **111**, 7431 (2007).
- ⁵⁴ S. L. Wang, C. M. L. Rittby, and W. R. M. Graham, J. Chem. Phys. **112**, 1457 (2000).
- ⁵⁵ A. D. Becke, Phys. Rev. A. **38**, 3098 (1988).
- ⁵⁶ J. P. Perdew, Phys. Rev. B **33**, 8822 (1986).
- ⁵⁷ C. Lee, W. Yang, and R.G. Parr, Phys. Rev. B **37**, 785 (1988).
- ⁵⁸ T. H. Dunning Jr., J. Chem. Phys. **90**, 1007 (1989).
- ⁵⁹ L. Lapinski and M. Vala, Chem. Phys. Lett. **300**, 195 (1999).
- ⁶⁰ T. F. Giesen, A. Van Orden, H. J. Hwang, R. S. Fellers, R. A. Provençal, and R. J. Saykally, Science **265**, 756 (1994).
- ⁶¹ D. Strelnikov, R. Reusch, and W. Krätschmer, J. Phys. Chem. A **109**, 7708 (2005).
- ⁶² J. Paldus, *Atomic, Molecular & Optical Physics Handbook*, Editor: G. W. F. Drake, (American Institute of Physics Press, 1996).

ABSTRACT

AN INVESTIGATION INTO THE LIMITATIONS OF THE HARMONIC APPROXIMATION IN THE CALCULATION OF VIBRATIONAL ISOTOPIC SHIFTS

by Guillermo García, Ph. D., 2008
Department of Physics and Astronomy
Texas Christian University

Dissertation Advisor:
Dr. C. Magnus L. Rittby, Professor of Physics

Comparisons between theoretical predictions and experimental measurements of vibrational fundamentals and isotopic shifts represent a method for the identification of new molecular species. For molecules with near-lying vibrational fundamentals, experimental and theoretical factors complicate the interpretation of isotopic spectra where isotopic shift measurements are recorded. Experimentally, a large number of absorptions in a small region of the spectrum are observed. Theoretically, two factors affect the calculation of isotopic shifts in the harmonic approximation: *i*) the sensitivity of the calculations due to the interaction of vibrational fundamentals and *ii*) the sensitivity of the calculations due to the anharmonicity of the interaction potential. The study of vibrational spectra of long carbon chains exhibits these problems.

The present work is an investigation of the theoretical issues that affect the calculations. As a consequence of this investigation, two theoretical methods were developed in the framework of perturbation theory in order to aid in the interpretation of

isotopic spectra of homonuclear molecules. Both theoretical methods are presented in this work. The first method, called the *isotopic deperturbation method*, is introduced in order to aid dealing with the complications regarding the sensitivity of simulated spectra due to the interactions of vibrational fundamentals. The second method is introduced here in order to estimate the anharmonicity of vibrational fundamentals from isotopic shift measurements.

The isotopic deperturbation method is applied to the infrared isotopic spectra of linear C_n ($n = 3 - 12, 15, 18$) and confirms our hypothesis regarding the high sensitivity of the isotopic shift calculation for molecules with near-lying vibrational fundamentals. The method to calculate anharmonic contributions is applied to the experimental spectra of linear carbon chains C_{2n+1} , $n=1-5$ as well as to cyclic C_6 and C_8 ; the results are compared with the calculated anharmonicity using a density functional theory (DFT) perturbative approach and existing calculations in the literature.

VITA

Guillermo García

Personal Background

Born August 25, 1978, Zacatecas, Zacatecas (Mexico)
The youngest son of Guillermo García Flores and Martha Navarro Pulgarín

Education

December 2000
B. S., Physics
UNIVERSIDAD AUTONOMA DE ZACATECAS (UAZ)

August 2008
Doctor of Philosophy, Physics
TEXAS CHRISTIAN UNIVERSITY (TCU)

Professional Presentations

A Deperturbation Method to Aid in the Interpretation of Infrared Isotopic Spectra, G. García and C. M. L. Rittby, 62nd Meeting of the International Symposium on Molecular Spectroscopy, The Ohio State University, Columbus, OH, June 2007.

A Deperturbation Method to Aid in the Interpretation of Infrared Isotopic Spectra, G. García and C. M. L. Rittby, TSAPS, University of Texas at Arlington, TX, October 2006.

Lyapunov Exponents for a Rainfall Time Series, G. García and A. Enciso, XLIII National Congress of Physics, Puebla, Mexico, November 2000.